

Abstract

Decommissioning of conventional power plants and the installation of inverter-based renewable energy technologies decreases overall power system inertia. This reduction in system inertia has an impact in the power system frequency response when an imbalance between generation and load occurs, increasing the rate of change of frequency (RoCoF) of the system. In a future scenario where renewables are predominant in power systems and due to the natural variability of the resource, imbalances of 40 percent or more are prompt to happen, when a system is islanded or operates as such, which combined with low inertia may lead to frequency collapse. This expected high values of RoCoF shorten the response time needed before load shedding and a subsequent possible black out occurs. Through the simulation of two scenarios with different primary reserve response, the requirements for the fleet of connected inverters was determined in terms of activation time and total power to be provided in order to avoid under frequency load shedding. This activation time was determined to be the time at which frequency would reach the load shedding value, known as critical time. With such value and knowing the time required for the synchronous reserve to deploy the imbalance power, a simple expression based on nullifying RoCoF at the critical time was obtained for the required inverter based fast power reserve. It was obtained that full activation time for inverter fast power reserve under 80% of penetration of inverter based generation would need to be between 50-500 ms for imbalances up to 40%; meaning that current frequency measurement techniques and renewable deployment times would not ensure system stability under the foreseen future possible power system conditions.

Introduction

As part of the international efforts set to counteract global warming, the deployment of renewable energies in the electric sector has been considered an energetic priority as a measure to reduce CO₂ emissions. This objective is also reflected in the regulatory energy policies and plans of some countries. For instance, in Germany the transformation of the electricity sector through renewables, known as “*Energiewende*”, contemplates to achieve a share in electricity consumption from renewables of 80 percent. As part of it, the renewable energy act, “*Erneuerbare Energien Gesetz*”, regulates the expansion of renewables and convectional generation decommissioning.

Even though power systems have grown in size and complexity, frequency control has been always performed through power balancing between generation and demand due to synchronous generator characteristics. The variation of load during a given period of time is followed by a change on the prime mover power of the synchronous generator. When an imbalance occurs, the excess or lack of power is injected to or released from the kinetic energy in the rotor. Therefore in synchronous grids, the magnitude of the rate of change of frequency (RoCoF) during an imbalance is inversely proportional to the system's inertia.

Decommissioning of convectional generating power plants and its replacement with inverter-based renewables power plants has as a consequence a reduction of system inertia and consequently increasing values of RoCoF. The relevance of system inertia is to avoid rapid changes in frequency as load-generation imbalance occurs; in this way enough time is given to the activation of primary power reserve to recover balanced stable conditions.

Therefore the need of new frequency control strategies is evident in this context; where inverter-based generation has a significant share in the grid. Due to the expected higher values of RoCoF, load shedding due to low frequency may occur faster than nowadays grid configuration. Hence, the participation of renewables in providing frequency support ancillary service is a key factor in achieving high integration of renewables without jeopardizing power system reliability.

So far, some ancillary services have been included in inverter's capabilities; inverter based generation from PV has been employed to contribute to voltage regulation by meanings of providing reactive power into the grid at cost of some active power. Similar approaches have been implemented for over frequency limitations, by curtailment implementation and ramping limitation of inverters when system frequency approaches an upper limit allowed by local codes. In the same sense, new techniques have been developed in order to enable inverter based generation, such as PV and Wind to participate also in frequency support for under frequency cases. The most common techniques try to emulate the droop power-frequency characteristic of the synchronous machine by leaving some power headroom during normal operation, so when a system frequency sag occurs, the inverter is able to push part or the total available power headroom to counteract the frequency drop. Hence

renewable sources are not any longer operating at its maximum power point, therefore these methods also have some economic constraints. Another approach to limit the frequency drop during the seconds after the event leading to a frequency decay, is to mimic the inertial response of synchronous machines. Since PV systems do not count with rotating masses, this approach is only achievable with wind turbines. Due to the decoupling of wind turbines from the grid dynamics, modified control strategies in the power electronics allows the controller to extract part of the stored kinetic energy in the rotating masses of the wind turbine.

In this Master Thesis the conditions, which should be fulfilled by inverters in highly penetrated grids by non-synchronous generation, to provide an inverter based fast power reserve (IBFPR) are investigated. Then the required triggering time and power response to avoid under frequency load shedding (UFLS) in such kind of islanded grids are estimated. The alternative of synthetic inertia is evaluated to see how effective it is under some assumed future scenario conditions. With the consideration of two cases, a micro-grid and electric island in the European scale; a methodology to determine the requirements of the fleet of inverters to offer frequency support is developed. The subsequent chapters will be covering the following content: Chapter 2 corresponds to the literature related to power system stability and primary reserve. Here an overview to the aspects behind the operation of typical power systems is presented, as well as how frequency is established and controlled. Additionally, the influence and contribution from inverter based generators is noted. Chapter 3 presents the methodology to estimate the power rate needed to avoid transient frequency instability. The developed method and expression for power rate are then evaluated in two cases: A micro-grid with fast primary reserve response and an electric island in a European scale with relative slow primary reserve response. A detailed demonstration of parameter setting and assumptions is presented as well. The results of the implemented method in each scenario is then shown in Chapter 4; critical times, frequency nadir and power responses are obtained. A detailed discussion of the main features and trends observed in the results section, is then followed in Chapter 5. Main conclusions and areas for future work are outlined in Chapters 6 and 7 respectively.

Theory

No matter the size or composition of the power system, a reliable and proper designed power system should fulfill some fundamental requirements (Kundur):

- The power system must have the capability of meeting the changing required load throughout time.
- Reduce costs and environmental impact.
- Ensure power quality and system stability (Voltage, frequency and level of reliability)

In conventional power systems, power balancing and frequency regulation is established through the control of synchronous machines power output. Although power systems capacities have increased along with their complexity for control and study, frequency control is implemented in the same way in any conventional grid.

Conventional Frequency Control and Stability

The balance between generation and load must be maintained so rotor speed and electric frequency are kept constant as described by the swing equation (Kundur; Anderson and Fouad). In order to achieve the before cited system conditions, a number of control devices and strategies must be implemented. Such controls must allow the system to remain in operation after small or severe events (change in loads, loss of generation units, faults...) maintaining frequency and voltage excursions under certain levels during transient conditions until steady conditions are reached.

Equation 1 represents the so called swing equation, where f_0 is the nominal system frequency, P_{mech} is the mechanical power from prime mover, P_{elec} is the electrical power demand, H is machine inertia constant and S_B is nominal power of the machine

$$\frac{df}{dt} = \frac{(P_{mech} - P_{elec}) * f_0}{2 * H * S_B}$$

Power balancing in synchronous generating units is performed by the governor of the prime mover coupled to the shaft of the generator.

As depicted in figure 1; conventional frequency control is comprised by three stages (Hansen et al. 2016):

- Inertia response: Subsequent to a power unbalance, power is subtracted or injected to the rotating mass of the rotor, creating a deaccelerating or accelerating torque in the shaft. This torque will decrease or increase rotor speed and frequency. The change

in frequency will be given by the amount of energy stored in the rotating masses (proportional to its inertia).

- Primary reserve: In a multi-machine system, all synchronous units contribute according to its capacity and droop characteristic. After the unbalance, the response time depends on governor control time. Once steady conditions are reached, an offset from the nominal frequency will remain as a consequence of the droop characteristics of the governors.
- Secondary reserve or Automatic Generation Control (AGC): This is coordinated from a central command (Transmission System Operator). Nominal frequency is restored from the deviation resulted from primary reserve implementation. This reserve do not necessarily comprises all connected generating units.

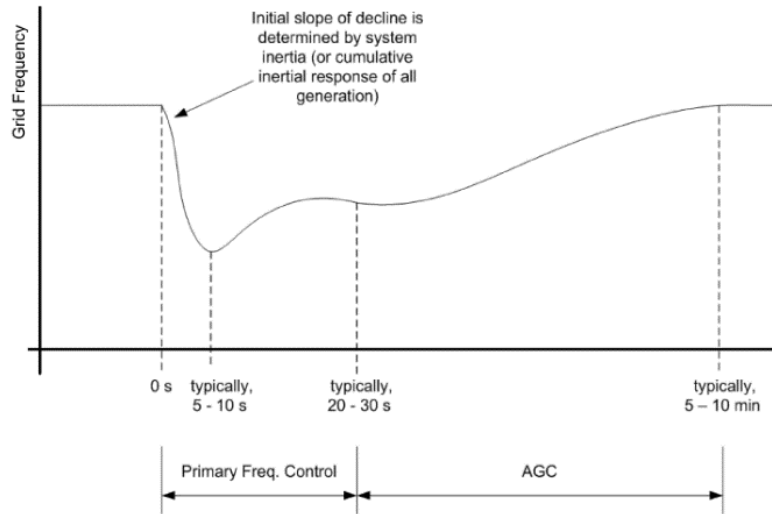
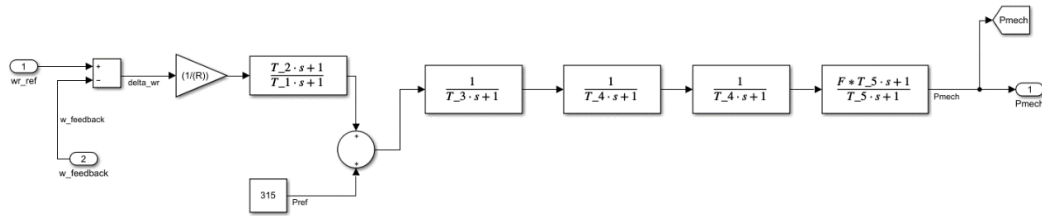


Figure 1: Frequency control in power systems (Aho et al. 2012)

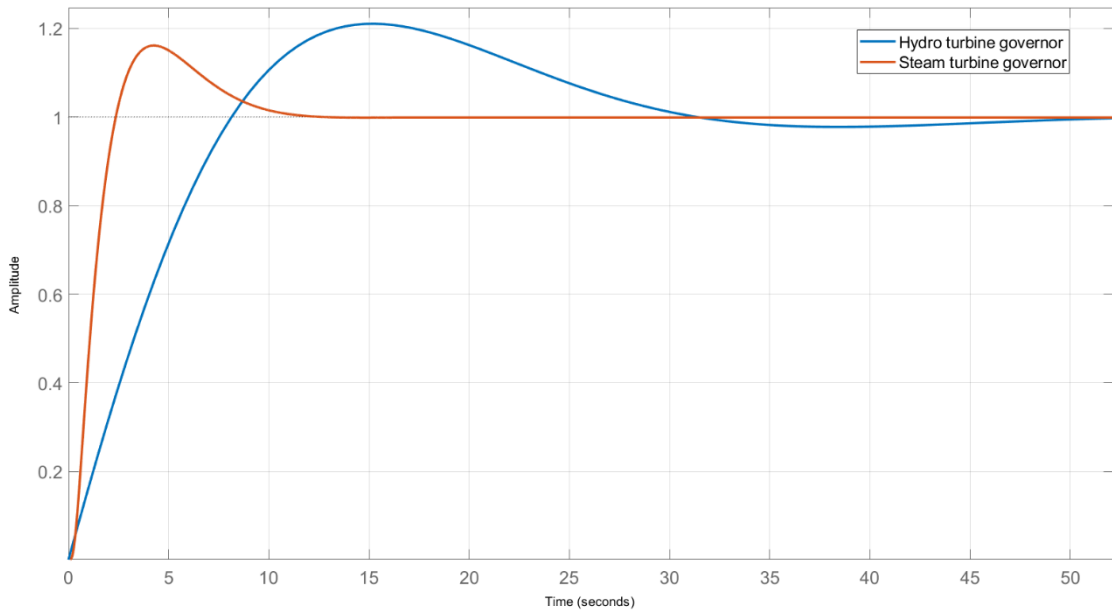
Primary Reserve Characteristics

Primary reserve requirements are different for each region or country. In Europe, ENTSOe establishes that the primary reserve must be equal to the size of the two biggest nuclear power plants. In this sense, a realistic scenario is considered. A bigger generation loss seems to be very unlikely. Commonly, primary reserve has a delay of a couple of seconds before it activates (2-5 s). As previously pointed out, during this time, inertial response from the rotating masses take care of slowing down frequency drop. In the European case, it is expected that the primary reserve is deployed completely in 30 seconds. This time is a common reference for primary reserve deployment. [Ref](#)

The characteristics of primary reserve are a combined response of the spinning generators online at the moment of a power unbalance. Each generator may present very different power response to changes in frequency. (ref) When single turbine-governor characteristics are considered a variety of responses could be achieved depending on governor model, settings and time constants. In order to explore the characteristics of steam and hydro governors, the model shown in figure XXX was used to determine its step response. Whether the model represents a steam or hydro turbine depends on the values selected for the time constants.



Where wr_{ref} is the nominal rotational mechanical speed in rad/s, $w_{feedback}$ the measured mechanical speed in rad/s, P_{ref} is the reference power in MW, R is the droop characteristic in pu and P_{mech} is the mechanical power output of the synchronous machine in MW.



When both models are compared, it can be noticed the faster response from the steam governor over the hydro governor. Even though steam turbines are less efficient when they are ramping power, it is shown that they can offer certain flexibility and fast governor response. On the other hand, hydro turbines have a slower response than conventional units.

Frequency Control with Distributed Energy Resources

Distributed Energy Resources (DER) in power system are mainly comprised by renewable energy resources. Currently one of the challenges in the implementation of DER as frequency control support is the lack of inertia response from them. As it was previously pointed out, inertia response is the first natural measure against the change in frequency when an imbalance occurs. In the case of PV systems, the generation of power is given by the photoelectric effect and no rotating masses are involved, having no inertia.

Additionally, given the inherent variability of renewable resources and technology characteristics (Asynchronous generation in variable speed wind turbines and DC power generation in PV), such technologies need the implementation of power converters which transform the unsuitable power output from the DER generators into suitable power to be injected into the grid. The power converter to be connected between the generator and the grid is in all cases an inverter; since it will convert the DC output of PV into AC synchronized power. In the case of variable speed wind turbines, the AC power with variable frequency is first converted to DC by rectifiers and then it is converted from DC to AC synchronized power output. This AC-DC-AC transition inhibits the wind turbine to react to grid disturbances. In general, it could be stated that the inertia of a power system is a measurement of its robustness, which means the higher the system inertia, the lower the rate of change of frequency (RoCoF) for a given system imbalance

Since the most prevailing inverter technology in grid connected DER is the grid-following type, frequency and voltage from the system are followed by the inverter, acting as a current source that operates at maximum power point, decoupling in this way the DER power production from the grid dynamics and disabling the participation of renewables without storage in power balancing and frequency regulation.

It is expected that grids with high penetration of DER to have a lower system inertia, leading to higher values of ROCOF. This high value of ROCOF can provoke big frequency excursions, having as possible consequence load shedding or even total system black out (ENTSOE 2016). Frequency is maintained in power system under very strict limits because sustained values out of the nominal range can cause severe mechanical damages in turbines and deterioration due to thermal effects and saturation in generators and transformers.

As synchronous machines installed capacity diminishes, not only the inertia of the system is reduced but also the contribution of synchronizing torque during disturbances. This can create small signal stability as well as frequency stability problems (Kroposki et al. 2017). Several novel approaches may be found in the literature for implementation of renewables in frequency regulation and inertia contribution. The main inertia control strategies are synthetic inertia and fast reserve power (Dreidy et al. 2017).

- Synthetic inertia: This control strategy applies only to wind turbines. This approach attempts to extract the kinetic energy from the rotating blades of the wind turbine when a disturbance occurs. Typically the control loop releases the kinetic energy based on the ROCOF and frequency deviation.
- Fast reserve power: In contrast to synthetic inertia, fast reserve power injects a constant amount of power during a certain amount of time through the control of rotor speed set point.

For frequency regulation, techniques such de-loading and droop control have been studied:

- De-loading: Wind turbines and PV plants typically operate at their maximum power point. That means obtaining the most of power from the primary resource (wind or solar irradiation), therefore when lack of generation occurs they cannot contribute to primary reserve for frequency regulation. In this approach the generators do not operate at their maximum power point but at a lower than maximum in order to allow the generator to operate at maximum when more power is required by the load.
- Droop control: Similarly to droop governors in synchronous machines, the control loop in wind turbines emulates the power-frequency dependency, allowing the turbine to react to changes in frequency with change in power output.

Frequency Measurement time and RE deployment time.

The current capabilities of non-synchronous technologies for fast power reserve are summarized in table XXX, additionally to such metrics, 100 ms for RoCoF measurement is noted [ref](#)

Technology	Full Fast Frequency response (ms)
Wind turbine-Synthetic inertia	~500
Lithium batteries	10-20
Flow batteries	10-20
Lead-acid batteries	40
Flywheels	<4
Super capacitor	10-20
Solar PV	100-200
HVDC	50-500

3 Methodology

As it was explained in chapter 2, the transitory frequency response of the system and therefore its stable and reliable operation after a perturbation, depends on the inherent characteristics of the power system (system inertia) and the counteraction measurements engaged automatically by the system (primary reserve). As the share of inverter based generation increases, the more prompt to instability the power system becomes. In this sense the added Inverter Based Fast Power Reserve (IBFPR) must be capable of maintaining transitory frequency value within the allowed limits.

Two terms commonly found in the literature of power system stability will be used along this section:

- Inertia constant H: It has units of seconds (s) and it is the ratio of the kinetic energy stored in the rotating masses of the generators (E_k in MWs) and its nominal capacity (S_{nom} in MVA).
- Acceleration time constant T_a : It also has the units of seconds (s) but this is the ratio of double the kinetic energy (MWs) and generators nominal power output (P_{nom} in MW).

With f as frequency, f_0 as nominal frequency and ΔP as power imbalance the swing equation can be expressed as follows:

Equation 3-1

$$\frac{df}{dt} = \frac{\Delta P * f_0}{2 * H * S_{nom}} = \frac{\Delta P * f_0}{T_a * P_{nom}} = \frac{\Delta P * f_0}{2 * E_k}$$

To describe the penetration of inverter based generation into the grid, these terms can be related to the overall power system. Even though the inertia constant H is most commonly used in the literature, the term of system acceleration time constant T_a is used instead when the penetration of non-synchronous generation in a power system is evaluated (ENTSOE 2016); this due to the fact it relates the load real power term (MW).

In this section the steps and methods applied in order to calculate the required Inverter Based Fast Power Reserve (IBFPR) to maintain frequency stability are presented.

Determination of IBFPR

Figure 3-1 depicts the typical frequency response when a negative power imbalance occurs in a power system. If the imbalance is high enough or the system inertia is too low, the initial ROCOF (XXX Maximum at beginning foot note) can lead to frequency excursions below the UFLS value. The value of ROCOF is brought to zero normally by the action of

the primary reserve; equalizing the power imbalance assuming no load frequency dependency. At this time the frequency nadir is reached as well.

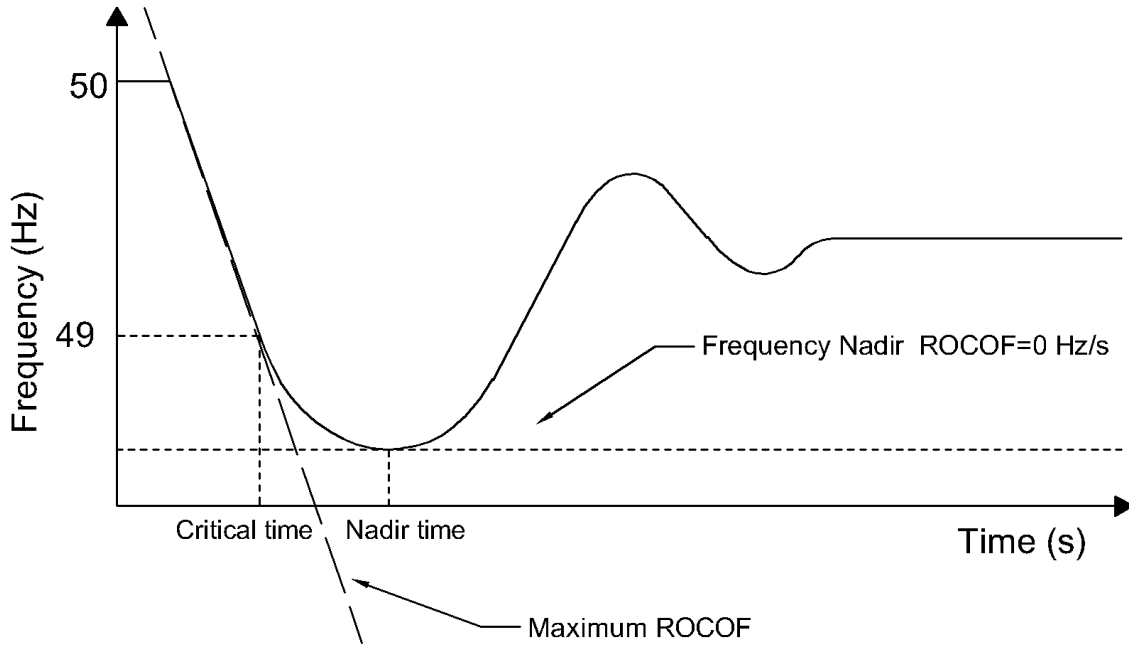


Figure 3-1: Frequency response of a typical power system subjected to a severe negative power unbalance.

When it is assumed that no load is rejected at UFLS frequency, the frequency continues dropping below 49 Hz. The time at which the system frequency equals the UFLS value is called in this thesis as critical time. This is the maximum available time for the inverter based reserve to deploy the required power to the system.

In the critical condition that would lead to load shedding, it is expected from the IBFPR to at least counteract the ROCOF at the critical time, as illustrated in **Figure 3-2**.

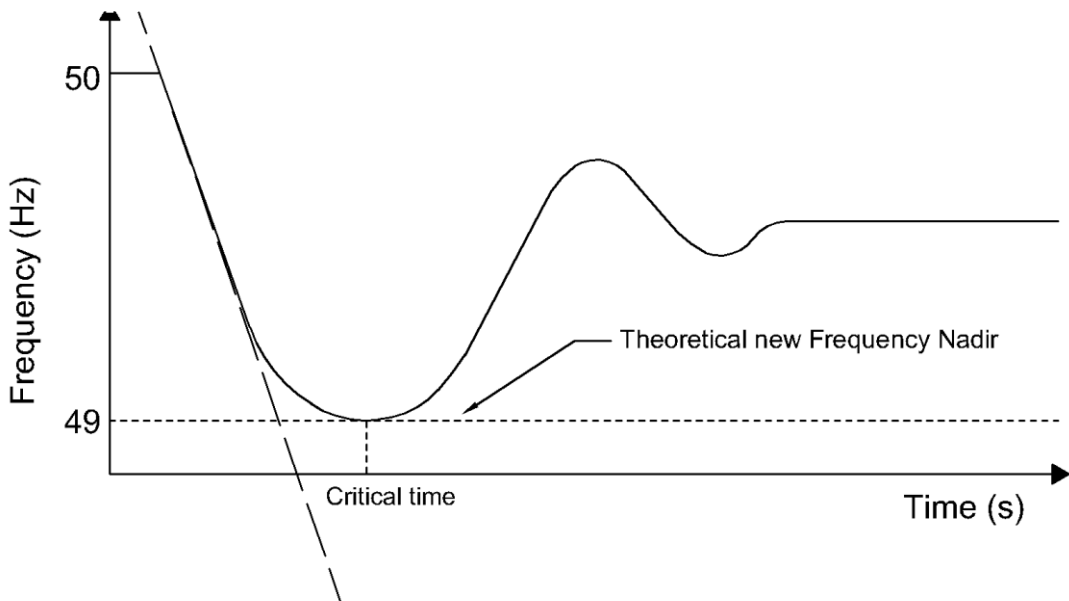


Figure 3-2: Expected power system frequency response with the addition of Inverter Based Fast Power Reserve.

Recalling equation 3-1; it is necessary that the machine's accelerating power (power imbalance) become zero at the critical time.

Equation 3-2

$$P_a(t_{cr}) = P_{mech} - P_{elec} + P_{IBFPR} = 0$$

Where P_a is accelerating power, P_{mech} is mechanical power, P_{elec} is electrical power (load), t_{cr} is the critical time and P_{IBFPR} is inverter based fast power reserve.

Typical primary power reserve response follows the indicated behavior shown in figure 3-4. Conventional turbine governor response is frequency dependent and may not respond linearly. For the estimation of IBFPR it was assumed a linear power deployment over time. Inspecting equation 3-1; it can be notice that only the power imbalance determines the rate of change in frequency in the system along with the kinetic energy stored in the rotating masses of the generators. For this reason the analysis is focused on the change on mechanical power after the event, ignoring the electrical load and mechanical power in the stable operation before the perturbation.

From the assumption of a linear mechanical deployment given from the synchronous machines governors, the rate of change in mechanical power, after a power imbalance ΔP , is given by $\Delta P/t_{nadir}$, where t_{nadir} represents the time at which the frequency nadir occurs. Given the power balance equation 3-2 at the critical time, t_{cr} ; the IBFPR response must be equal to $P_{elec} - P_{mech}$, being P_{elec} equal to ΔP .

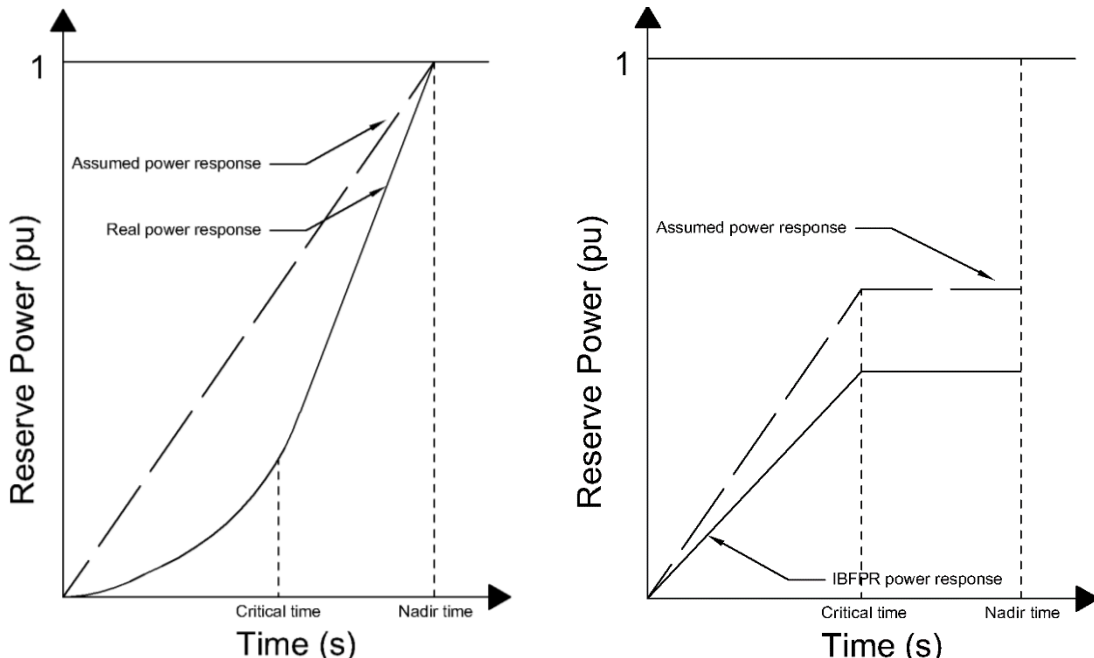


Figure 3-4: Comparison of assumed power reserve deployment and typical real response. Figure 3-3: Assumed primary power reserve and IBFPR.

Substituting P_{mech} by $\Delta P * t_{cr} / t_{nadir}$ and P_{elec} by ΔP in equation 3-2, the following expression is obtained for the P_{IBFPR} at time t_{cr} .

Equation 3-3

$$P_{IBFPR}(t_{cr}) = \Delta P * \left(1 - \frac{t_{cr}}{t_{nadir}}\right)$$

It is assumed that P_{IBFPR} remains with a constant power output after t_{cr} long enough to stabilize the system frequency. The result of the previous equation represents the slope of the power output since the inception of the incident until the critical time, which with the implementation of IBFPR, it will be not any longer critical but rather it will be the new desired frequency nadir time.

Equation 3-4: IBFPR before critical time.

$$P_{IBFPR}(t) = \frac{\Delta P}{t_{cr}} * \left(1 - \frac{t_{cr}}{t_{nadir}}\right) * t$$

According to the obtained expression; it can be realized that the desired power response from the inverters depends exclusively on parameters which cannot be directly measured from the grid connection point. In a real situation the values of ΔP , t_{nadir} and t_{cr} cannot be known in advance, representing this factors a challenge in the implementation of this ideal power response. Those values are dependent on the grid characteristics; depending on the primary conventional reserve deployment time and the overall system inertia. Thus two main cases are considered for the remaining analysis with the intent of covering a wider range of systems with different characteristics.

3.1 Cases for Assessing IBFPR

As presented in the previous section, the values of critical time and frequency nadir time depend on the system imbalance and primary reserve deployment time. In chapter 2 it was illustrated the different governor response for different primary reserve type. To be able to assess the influence of the grid size and the primary reserve characteristics, two main cases were considered.

- Micro-grid Case: For the evaluation of this case; typical governor data is considered in a well-known and studied benchmark grid topology as the WSCC model, also known as the IEEE 9 bus model. Synchronous activation in the order of ~ 3 s.
- European island Case: In the European island scale all synchronous machines are modeled and simplified as one single machine, provided with the characteristic expected from the overall system. Synchronous activation in the order of ~ 30 s.

Micro-grid Case-IEEE 9 bus model

Microgrids can operate connected to the bulk transmission/distribution system or stand alone. In any case, it is assumed that imbalances could occur due to internal faults when island configuration is considered or islanding from the whole system is result from a contingency while most load power of the microgrid was being ‘imported’. For the study of power systems and the increasing interest in stability analysis in microgrids, the IEEE benchmarks represent a widely used option, based on some real data; this is also the case of the IEEE 9 bus model or WSCC (Western System Coordinated Council). The IEEE 9 bus model is a representation of the former western interconnected power system of North America of 1967. For stability and reliability studies, this system has been employed in many publications as study case (Atieh Delavari et al.), which allows the comparison of results. **Figure 3-5** illustrates grid’s configuration. Detailed grid parameters are found in Appendix XXX ref

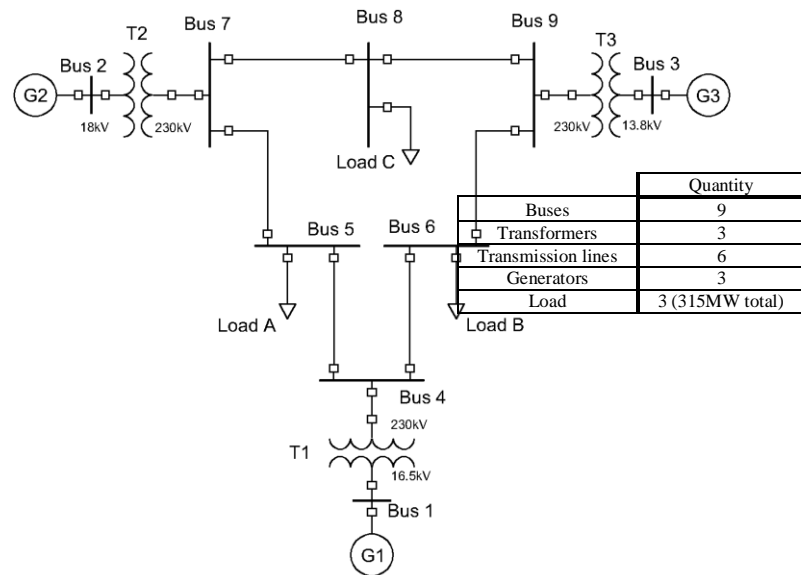


Figure 3-5: WSCC or IEEE 9 bus model used for stability studies.

As a first step to evaluate the impact of inverter based generation and power imbalances in the grid, the whole system is simplified as one single generating unit; neglecting all losses in the system (Transformers, transmission lines and generators) with the assumption that the mechanical output of the prime mover is the same than the electrical power output at generator terminals. A schematic representation of such system is presented in **Figure 3-6**.

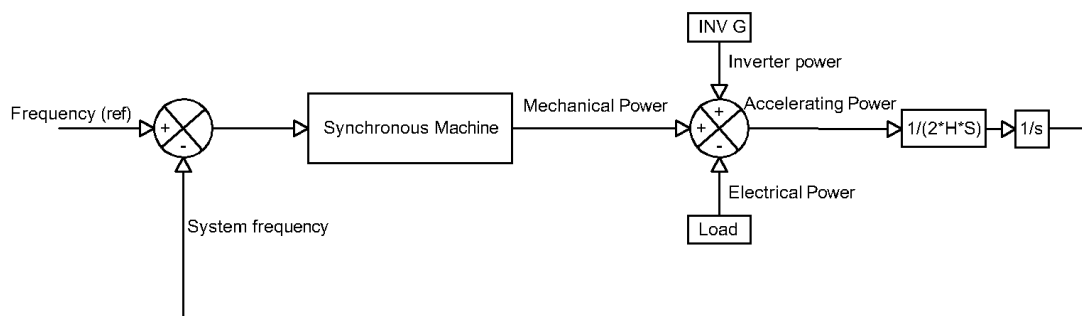


Figure 3-6: Single machine representation of the IEEE 9 bus model.

The governor model presented **Figure 3-7** is used to represent the simplified synchronous machine. Although there are plenty of options for governor modelling; the selection of such model was based on the availability of the typical time constants according to generator capacity (Anderson and Fouad 2002). Additionally, depending on the selected parameters, the model can be used as steam or hydro governing system. The step response of the governor model under a three different penetration of non-synchronous generation is presented in **Figure 3-8**. From that, activation time is between 1.14-3.24 s (nadir time).

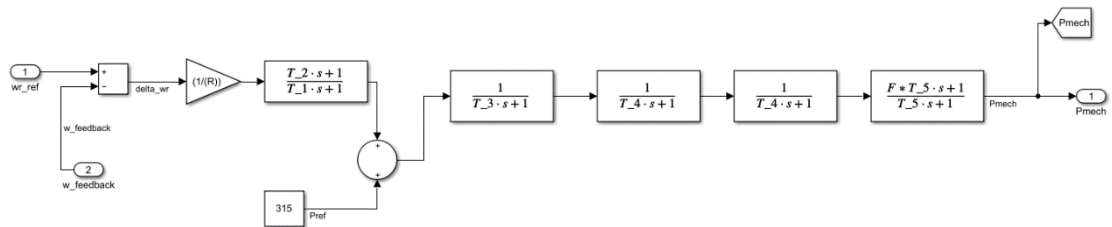


Figure 3-8: Governor representation implemented as synchronous response in the system.

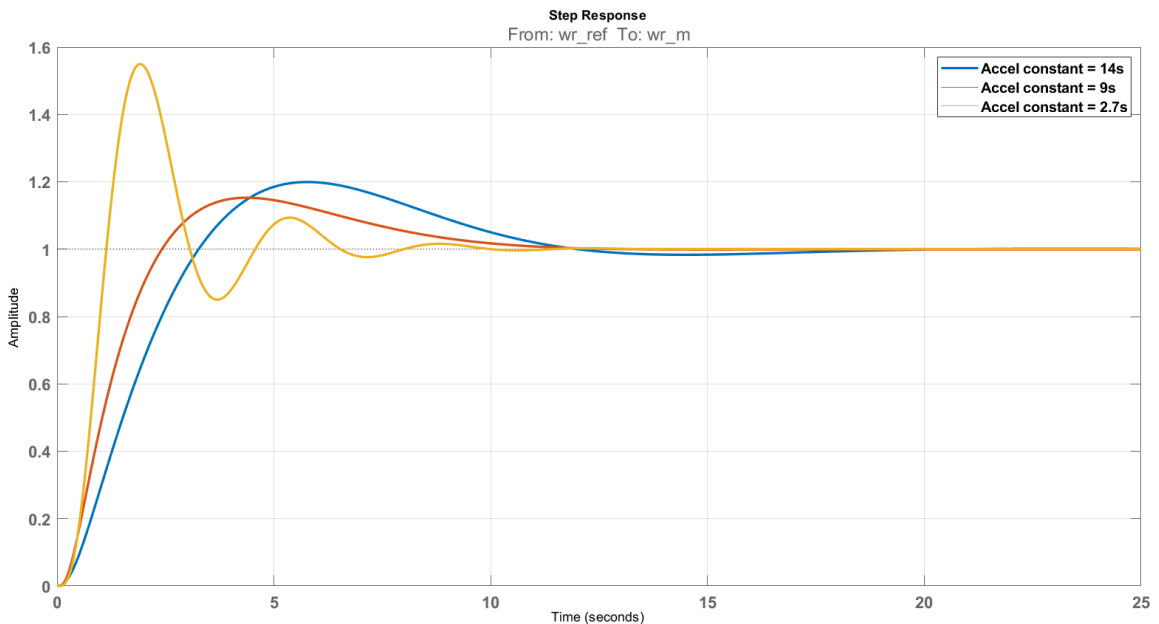


Figure 3-7: Step response of Governor model for different values of acceleration time constant.

The values of kinetic energy and time constants of a synchronous machines of 835 MVA were selected to represent the synchronous response, with the load of 315 MW the system acceleration time constant is 14 s (ref), which is approximately today's Europe acceleration constant (ENTSOE 2016). This is the base scenario, assuming 100% synchronous generation. To evaluate the impact of the penetration of inverter based generation; the values of lower capacity generators were selected (ref), assuming the compensation of the remaining power by a constant power source representing the inverter based generation, decreasing in this manner the total system acceleration time constant, thus the kinetic energy of the generator. Up to this point, neither synthetic inertia nor frequency support

from renewables is considered. Inverter based power output remains constant before, during and after the perturbation. Therefore the system imbalance is covered only by the synchronous equivalent machine.

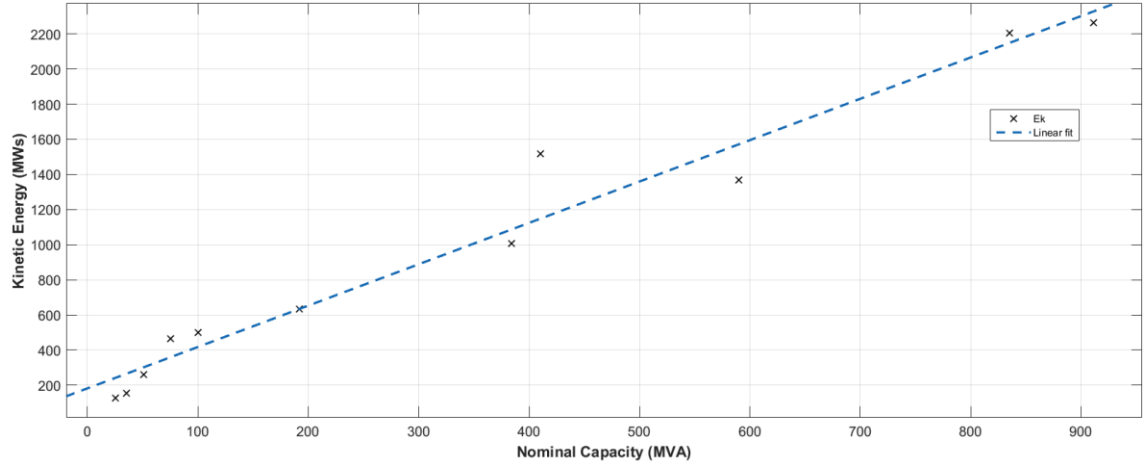


Figure 3-9: Kinetic energy stored in generator rotating masses as function of generator capacity. A linear relation is exhibited between the machine capacity and its store kinetic energy.

Even though load imbalances up to 40% were simulated in each inertia scenario, the power capacity limit of the generators was disregarded for estimation of the critical time. The negative imbalance was simulated by increasing the system load by the corresponding factor. A block diagram representing the system in the given conditions was designed in MATLAB-SIMULINK. With the help of a MATLAB code several simulations were run and the critical and nadir times acquired for each scenario. With the calculated times, the IBFPR to avoid load shedding under each scenario was calculated as given by [equation 3-4](#) and it is shown in the Results section.

All the acquired values of critical time, as result from the simulations, are then related with the system ROCOF, so a regression can be performed and link the critical time with system ROCOF.

For the system conditions and the employment of the fitting tool provided by MATLAB, an expression is obtained for critical time as a function of ROCOF.

As it will be detailed shown in the result section, for unstable conditions the maximum critical time is 2.7 seconds. Therefore critical time must be lower or equal to that value; calculating in this way that the minimum ROCOF for activation as 0.6143 Hz/s.

Implementation of IBFPR in the IEEE 9 bus model

In order to test the values found of power response from the inverters, these are implemented through a simple SIMULINK algorithm which estimates the power imbalance and critical time based on the measurement of the ROCOF, when system inertia it is known. Based on those estimated values, the algorithm provides the power ramp before the calculated critical time is reached and maintain constant power output after this time.

The algorithm works in a simple way:

1. It measures the system ROCOF.
2. If the value exceeds 0.6143 Hz/s the IBFPR is activated.
3. According to the measured value of ROCOF and available system inertia, a ramp power response is injected into the system during a time equal to the calculated critical time according to **equation 3-4**. Critical time calculated from fit.
4. When the calculated critical time is reached, the IBFPR must stop ramping power and keep a steady value until frequency is restore to an acceptable value as per **equation 3-3**.

The block diagram is provided in Appendix XXXX

Synthetic Inertia in the IEEE 9 bus model

Synthetic inertia was explained in chapter 2 as one of the new techniques that manufacturers and researchers are considering to tackle with the low inertia problem in power systems (General Electric International 2013) (Dreidy et al. 2017). Frequency support through synthetic inertia was considered with the following assumptions (Dreidy et al. 2017):

1. Power output from synthetic inertia is limited to 10% of wind turbine nominal power.
2. Due to mechanical and thermal stresses, the additional power can be delivered only for a maximum time of 10 s.
3. It's assumed that all wind turbines operate at its maximum power output. The value of 1.5 MW was selected for such purpose.
4. In order to avoid wind turbine stall, the removed kinetic energy from the blades (injected to the grid in electrical form) it is limited to half (E. Muljadi, V. Gevorgian, and M. Singh: NREL and S. Santoso: University of Texas - Austin 2012).

To be able to extract energy from the rotating blades of the wind turbine, an adequate control system is needed. From the expression of power as the derivative of energy and the kinetic energy stored in the blades, the rate of energy extracted from the wind turbine can be obtained, considering that rotational speed changes in time.

$$P = \frac{dE_k}{dt} ; \quad E_k = \frac{J_{wt}*w^2}{2};$$

$$P = \frac{J_{wt}}{2} * \frac{dw^2}{dt}$$

$$J_{wtc} = \frac{2 * H_{wt} * S_{wtc}}{w^2}$$

Equation 3-5

$$P_{pu}(t) = 2 * H_{wt} * w_{pu}(t) * \frac{dw_{pu}(t)}{dt}$$

Where E_k is kinetic energy, H_{wt} is the turbine inertia constant, w the rotational speed and J_{wt} the turbine inertia.

Equation 3-6 represents the rate of change of kinetic energy extracted from the rotating masses of the wind turbine in pu. The implementation of such equation in SIMULINK is shown in **Figure 3-10**. Additionally, a gain block K_i was added in order to inject more power from the very beginning of the power imbalance. A filter at the signal entrance was added in order to suppress non desired oscillations on the system (General Electric International 2013).

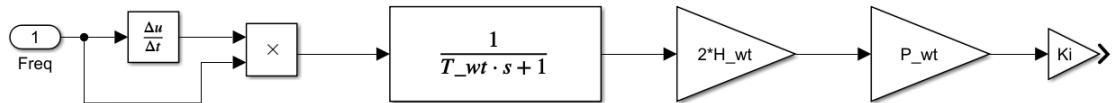


Figure 3-10: Synthetic inertia control model where T_{wt} is the filter constant, H_{wt} is the turbine's inertia constant, P_{wt} is the nominal wind capacity (MW) and K_i is a gain constant. Frequency input in pu and system output is power in MW.

Typical values for inertia constant of wind turbines are not openly available from the manufacturers to the public. Hence an approximate value was calculated with the utilization of an equation which relates nominal power and inertia constant for wind turbines (González Rodríguez et al. 2007).

Equation 3-6: Wind turbine inertia constant as function of the nominal power in MW.

$$H_{wt} \cong 1.87 * P_{nwt}^{0.0597}$$

For a wind turbine with nominal power output of 1.5 MW the value of H corresponds to 4.37s, which is in an acceptable range (Wu and Infield 2013).

It is assumed that all the wind turbines, when operating, are delivering their nominal power output. A nominal rotational speed of 18 rev/min was considered (Wu and Infield 2013). To avoid the wind turbine to stall, only a reduction of 5 rev/min it is allowed by the implementation of the control system. This change of rotational speed equals a change of 3 MWs reduction on kinetic energy out of a total of 6 MWs.

T_{wt} (-)	H_{wt} (s)	P_{wt} (MW)	K_i (-)
1	4.37	$1.5*n_{wt}^{-1}$	10

Synthetic Inertia and IBFPR in the IEEE 9 bus model

In this model the contribution to system frequency stability of both models operating together is evaluated as shown in **Figure 3-11**. No additional modification or adjustment was performed to the IBFPR or the synthetic inertia model.

Procuring to estimate frequency measuring time influence, an intentional delay was introduced to the IBPFR and the SI response. This delay emulates the required time for frequency measurement, filtering and signal processing. A delay transport block was added in the power response. Depending on the technique and precision desired, the time for acquiring frequency reading may differ considerably, however, for the purpose of this research the time of 100 ms with an error of 5 mHz was taken as the fastest measurement reading time. [ref](#)

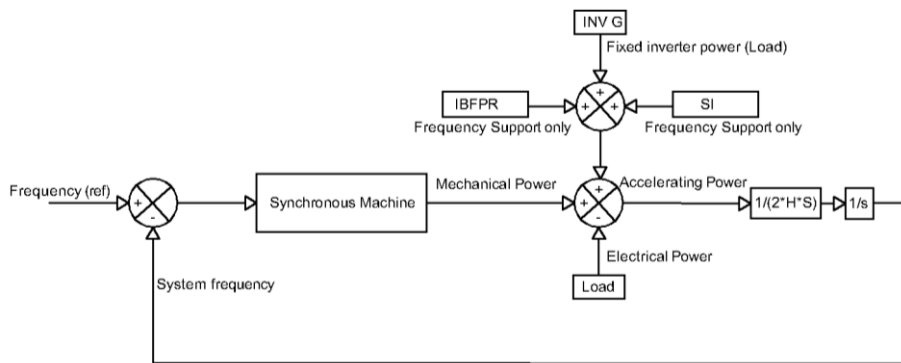


Figure 3-11: Synthetic inertia and IBFPR implementation.

Analysis of the insertion of multiple machines in the simulation

It was previously stated that in the first approach, only the total load was considered in the simulations as well as the synchronous generation represented by one single machine and no system losses. Since it is desired to compare the results of the system with such simplifications against some model that takes into account the whole system components, losses and dynamics; A SIMSCAPE-SIMULINK representation of the IEEE 9 bus model was implemented (Atieh Delavari et al.). In this representation, simulations for different values of system inertia and load imbalance were performed, similarly as it was done with the simplified block representation of the model.

In order to evaluate the validity of the equation describing the IBFPR needed to avoid ULFS, the SIMSCAPE model was modified with the insertion of ideal controlled power sources blocks, which were set up to inject power into the grid accordingly to the simulated scenario. Therefore, no means of frequency measurement were included and only IBFPR was assessed.

System settings for stability study.

Since it is desired to compare the complete representation of the IEEE 9 bus model against the simplified model representation; it is assumed in the same manner that the total acceleration time constant of the system equals 14s, similarly as in the block representation. Hence the same kinetic energy should be distributed among the three generator's rotating masses in the SIMSCAPE model as in the simplified representation. From [equation 3-8](#) for system acceleration time constant, it can be easily calculated that the system kinetic energy with 14 s (100% synchronous generation) is 2205 MWs.

Equation 3-7

$$T_{sys} = \frac{2 * E_k}{P_{LOAD}}$$

Due to the fact that inverter based generation reduces the system kinetic energy; for different levels of inverter based generation, the generators nominal capacities (S , MVA) values were kept constant and the inertia constant (H , s) of each machine multiplied by the synchronous share factor (f_{ss}). Total system kinetic energy is the summation of all units together. In this way, the synchronous generators in the initial state of equilibrium represent both power sources, inverter based plus synchronous.

Equation 3-8

$$E_k = 2 * (H * f_{ss}) * S$$

Prime mover and governor

The type of prime mover selected was conventional steam turbines and its governor system. Steam governor and turbine representation in SIMSCAPE block is presented in [Figure 3-12](#)

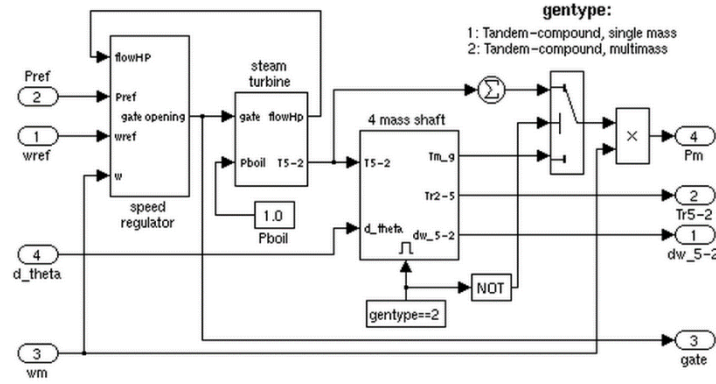


Figure 3-12: Governor and steam turbine model from SIMSCAPE library

The block contains a complete tandem-compound steam prime mover, including a speed governing system, a four-stage steam turbine, and a shaft with up to four masses. The speed governing system consists of a proportional regulator, a speed relay, and a servomotor controlling the gate opening. The steam turbine has four stages, each modeled by a first-order transfer function. The first stage represents the steam chest while the three other stages represent either reheat or crossover piping. The boiler is not modeled and boiler pressure is constant at 1.0 pu. Additionally, an exciter system was added to the machines, the parameters of such blocks as well as turbine constants are presented in APPENDIX

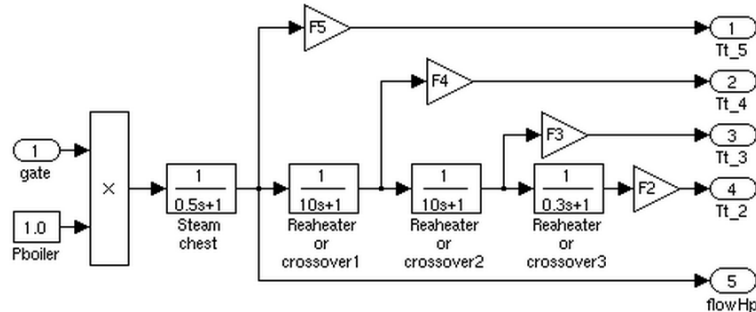


Figure 3-13: Steam turbine model

In order to start the simulations in steady state, a load flow calculation of grid must be carried out with the objective of calculate the initial conditions for the exciter and prime mover models. Table XXX summarizes the main values for setting system initial conditions; acquired from the power flow tool provided by SIMSCAPE.

Bus number	Bus type	Voltage	Power	Reactive Power
		Per unit	MW	MVAr
1	Slack	$1.04 \angle 0^\circ$	72.2	25.64
2	PV	$1.025 \angle 9.83^\circ$	163	8
3	PV	$1.025 \angle 4.63^\circ$	85	-9.41
5	PQ	$0.9949 \angle -4.42^\circ$	125	50
6	PQ	$1.01211 \angle -4.16^\circ$	90	30
8	PQ	$1.0172 \angle 0.17^\circ$	100	35

IBFPR representation

Similarly as it was done in the simplified block model, a subsystem is implemented in the SIMSCAPE model in order to represent the IBFPR and analyze the system behavior with the addition of this power. To do so, the IBFPR was modeled as controlled current sources; such controlled sources inject active power according to the load imbalance and system inertia simulated. Continuous voltage measurement is required in order to determine the amount of current needed to supply the requested power. **Figure 3-14** depicts the schematics of the IBFPR control.

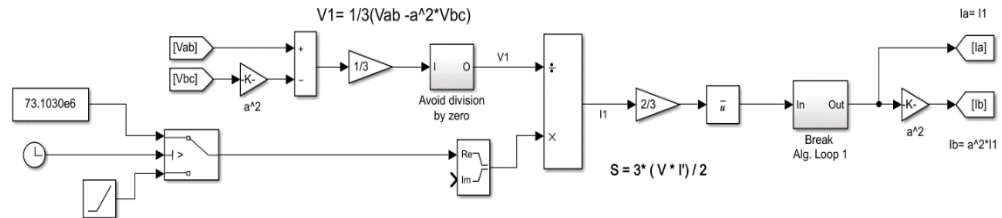


Figure 3-14: Model implemented to calculate the required current to meet the specified power rate.

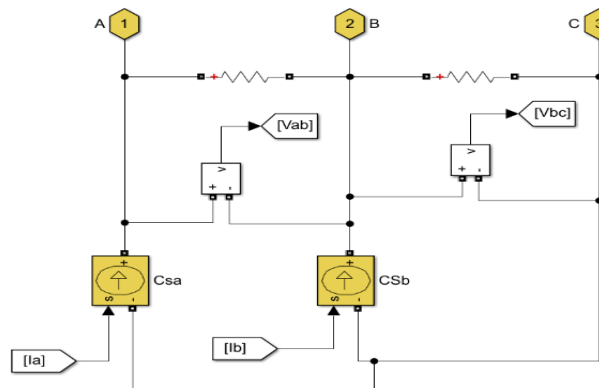


Figure 3-15: Controlled current sources acting as grid following inverters. Signals I_a and I_b comes from model in figure 3-14; similarly signals V_{ab} and V_{bc} go to the same model.

It can be noticed from **Figure 3-15** that the IBFPR is composed of 2 current sources, 2 voltage readers (complex measurement), two resistance and 3 connecting ports.

The IBFPR will have symmetrical and balanced characteristics. Due to this reason, the magnitude and angle of the current phasor will be obtained from the positive sequence of the measured voltage, since unsymmetrical line voltages may be present on the system.

Given a symmetrical IBFPR; only two current sources are needed because the addition of balanced currents in a three phase system equals 0. Hence, leg c will be fed with the negative of the sum of both sources.

$$I_a + I_b + I_c = 0$$

$$I_c = -I_a - I_b$$

The ports are connected at the medium voltage side of the system (generator's side). The resistance must have a high value (negligible current flowing through); this is a requirement for the implementation of SIMSCAPE current sources.

Figure 3-14 shows the block diagram implemented to obtain the positive symmetrical component of line voltage and the positive sequence of current that will be provided by the subsystem. From the definition of complex power and voltage symmetrical components in three phase systems, the positive sequence component of phase voltage and line current are obtained. The positive sequence component of complex power is equal to the complex balanced power (ref power system analysis):

Equation 3-9

$$S_{3\omega}^I = 3 * V_{LN}^I * \overline{(I_L^I)}$$

This equation is valid for RMS values of voltage and current; nevertheless the measured voltage values and the sought current values are given in peak values, the equation for power and current become:

Equation 3-10

$$S_{3\omega}^I = \frac{3 * V_{LNpeak}^I * \overline{(I_{Lpeak}^I)}}{2}$$

Equation 3-11

$$I_{Lpeak}^I = \sqrt{\frac{2 * S_{3\omega}^I}{3 * V_{LNpeak}^I}}$$

With the help of the **a** operator ($-0.5+j\sqrt{3}$ or $1\angle 120^\circ$) the values of the positive sequence component of phase voltage can be obtained.

From $V_a + V_b + V_c = 0$ and $V_a^I = (1/3) * (V_a + aV_b + a^2V_c)$

$$V_a^I = (1/3) * (V_a + aV_b - a^2V_b - a^2)$$

$$V_a^I = (1/3) * \{V_a * (1 - a^2) + aV_b * (1 - a)\}$$

Since $V_{an}^I = \frac{V_a^I}{\sqrt{3} \angle 30^\circ}$, $\sqrt{3} \angle 30^\circ = (1 - a^2)$ and $\sqrt{3} \angle -30^\circ = (1 - a)$ then after some algebraic manipulation the expression for V_{an}^I becomes:

Equation 3-12

$$V_{an}^I = (1/3) * (V_a - a^2V_b)$$

With the obtained expressions for the positive sequence of phase voltage and complex power, the needed current to supply the IBFPR related to the measured voltages can be implemented. The ramping function will last until the critical time is reached, afterwards, the IBFPR output will remain constant.

European Case

Under normal operation ENTSOE has reported values of ROCOF in the range of 5-10 mHz/s for power outages of 1 GW in the current interconnected power system. If an imbalance event of more than 3 GW occurs with depleted primary reserve, extraordinary values of frequency and ROCOF might be reached. After serious disturbances the Continental European Power System has experienced ROCOF between 100 mHz/s and 1 Hz/s. Imbalances of 20% or more along with ROCOF greater than 1 Hz/s have been determined by experience to be critical (ENTSOE 2016).

ENTSOE has determined that under the case of the reference scenario (The loss of 3 GW generation with 150 GW load and 2%/Hz self-regulation) in the interconnected operation, the influence of inverter based generation, and therefore the reduction of system inertia would not jeopardize system stability. Due to the expected increase of non-synchronous generation in the future, international power trade and renewables variability; ENTSOE estates in its split reference scenario that the power system must be capable of withstanding imbalances greater than 40% with ROCOF of 2 Hz/s or higher. Under these circumstances the resulting islands must avoid load shedding. Hence, only the split scenario is considered for further analysis.

When considering the system blackout of November 4th 2007, in which four electric islands resulted from the European system split; system blackout due to underfrequency was experienced in the so known western area. This island, at the moment of split, had approximately a load of 190 GW (27% more than the low load ENTSOE scenario). For it comparable ‘size’ and the uncertainty of knowing beforehand the resulting islands after a major contingency, the selected load for simulation was the same as the ENTSOE reference scenario as well as the primary reserve deployment time.

To simulate the behavior of the resulting island in the European split scenario; a simplified approach was selected. Similarly as it was done with the simplified block model for the IEEE 9 bus model, in the equivalent European representation all the synchronous generation will be represented by a single machine, which will provide governor response when a perturbation takes place. Additional to the synchronous response, a load response of 2% was added to the model, which means that for every Hertz reduced or augmented, the load will reduce or increase by a 2%.

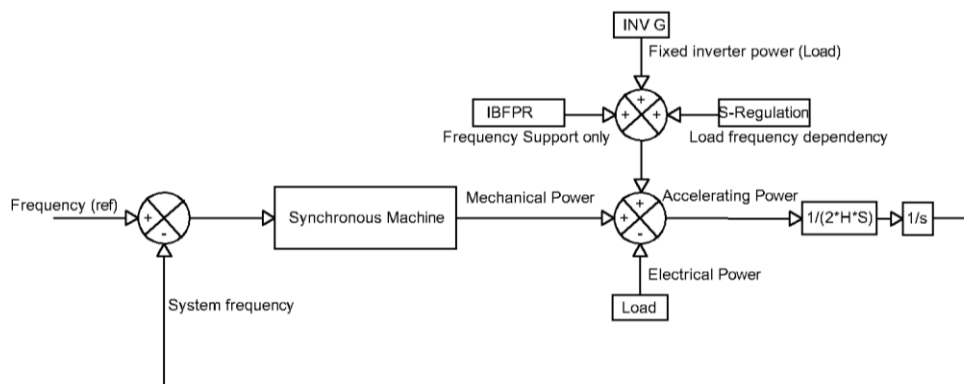


Figure 3-16: Simplified European power system.

Figure 3-17 depicts the results of ENTSOE for the interconnected reference scenario frequency response model. It is intended that the implemented model for the island would perform in a similar way like the ENTSOE model for the same conditions.

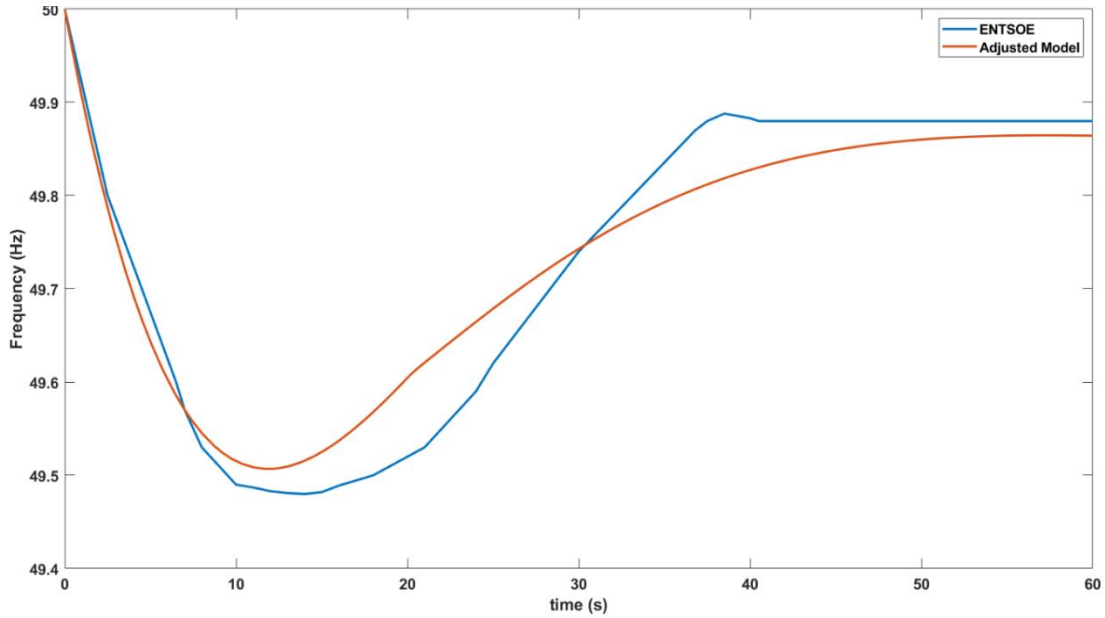


Figure 3-17: Comparisson between the modeled reference scenario by ENTSOE and the adjusted model. Power loss of 3GW, load of 150 GW (2%), self-regulation of 2%/Hz and acceleration time constant of 10 s.

To fit the behavior of the system to the modeled by ENTSOE, a PID controller was added in the SIMULINK micro-grid model to the steam turbine governor; this was done with the intention of adjusting the time response of the primary reserve as much as possible to the desired one. With the PID approach, the primary power reserve can be easily tuned with the assistance of the PID tuner app available in MATLAB. The period of time of utmost interest for analysis is from the inception of the power imbalance and the nadir time. Therefore, the system must perform as similar as possible in this region compared to the ENTSOE reference, whereas after the nadir time, the disparity between responses can be neglected. In the European scale the reserves must be completely deployed within 30 s after the occurrence of the disturbance.

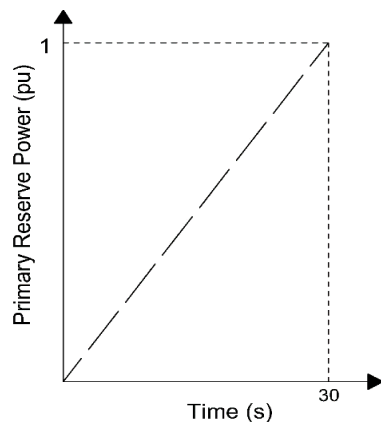


Figure 3-18: Primary reserve deployment time of the interconnected European system

System parameters

A power system of n number of synchronous machines is assumed; having each of them a capacity S in MVA, a nominal power P_n in MW and a nominal power factor.

Assuming that each machine operates at a de-load factor dl of P_{nom} ; with an acceleration constant equal to T_{nom} then the number of machines n , for the synchronous load P_{load_sync} is:

Equation 3-13

$$n = \frac{P_{load_sync}}{P_{nom} * dl}$$

Then the time acceleration constant of the system T_{sys} can be obtained as follows:

$$T_{sys} = \frac{\sum_i^n P_i * T_i}{P_{LOAD}}$$

$$T_{sys} = \frac{n P_{nom} * T_i}{P_{LOAD}}$$

$$T_{sys} = \frac{P_{load_sync} * T_{nom}}{P_{LOAD} * dl}$$

Equation 3-14

$$T_{sys} = \frac{\text{Sync share} * T_{nom}}{dl}$$

In this sense the base system time acceleration constant (synchronous share 100%) is calculated from the values of $T_{nom}=10$ s, synchronous share $\text{Sync_share}=1$, and a de-load factor $dl=0.8$ having as a result $T_{sys}=12.5$ s

The values of the PID controller and the step response characteristics of the model are summarized in **table XXX**. Step response before and after PID tuning can be observed in **Figure 3-19** and **Figure 3-20**.

Considering only the swing equation, as done in the model, it can be demonstrated that the ROCOF and therefore the frequency response of the system is only dependent on the percentage of load imbalance and the system acceleration time constant.

From the definition of ROCOF as $\frac{df}{dt} = \frac{\Delta P * f_0}{2 * E_k}$ and $T_{sys} = \frac{2 * E_k}{P_{LOAD}}$:

$$\frac{df}{dt} = \frac{\Delta P * f_0}{P_{LOAD} * T_{sys}}$$

Equation 3-15

$$\frac{df}{dt} = \frac{\Delta P_{pu} * f_0}{T_{sys}}$$

In equation 3-16, the value of ΔP_{pu} is the normalized value of power imbalance having as base power the value of load P_{LOAD} . As shown in the equation, when only the swing equation is considered, the frequency response is only dependent on system acceleration constant and the relative value of imbalance. This relative value of imbalance varies during time, depending on load response to change on frequency and the response of primary reserve of the system.

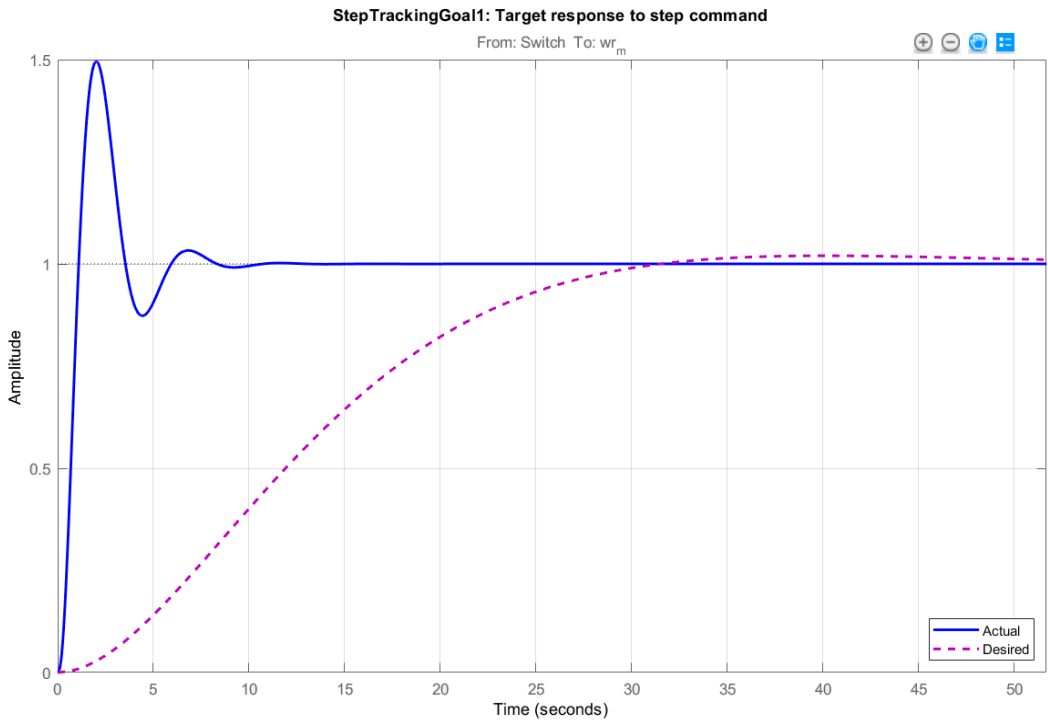


Figure 3-19: Comparison between system step response before the PID tuning (blue) and the desired step response of the system (pink).

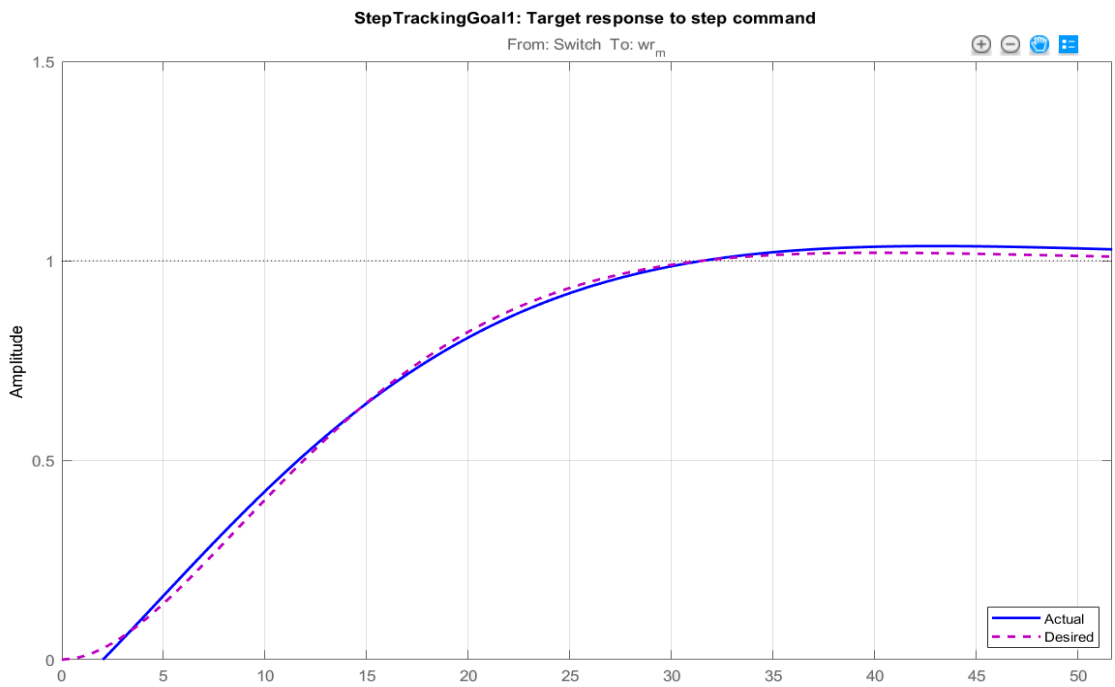


Figure 3-20: Comparisson between the actual response (blue) and the desired step response of the system (pink); after PID tunning.

Scenario Summary

Micro-grid IEEE 9 bus model

Implementation of individual governor response to generators.

Case A-Simplified block model: One machine, one load and no losses representation to the IEEE 9 bus model.

- Determination of critical time.
- Determination of IBFPR and impact of SI and frequency measurement delay in frequency response.

Case B-Multimachine system: Detailed model; every main component and its dynamic model of the benchmark is considered.

- Determination of critical time.
- Analysis of the Machines interaction with IBFPR model.

European Scale

Case-Split operation: Analysis with imbalances up to 40% with variation of primary power reserve deployment in 30 s in an islanded system. Island frequency response is assumed to be the same that the European response analyzed by ENTSOE.

- Determination of critical time.
- Determination of IBFPR and impact of SI and frequency measurement delay.

4 Results

In this section the main results of the cases described in the former section are presented. The results are presented by subsections according to the specific cases:

Micro-grid Case- Simplified IEEE 9 bus model

Determination of critical time

The simplified block representation of the IEEE 9 bus model presented in chapter 3 was used to determine the critical times; for which the inverter based generation must supply the ramping power in order to avoid frequency instability. **Figure 4-1** depicts the range of critical time depending on the combination of system inertia (Acceleration time constant) and power imbalance. It is well to note that the absolute values of RoCoF and power imbalance where considered.

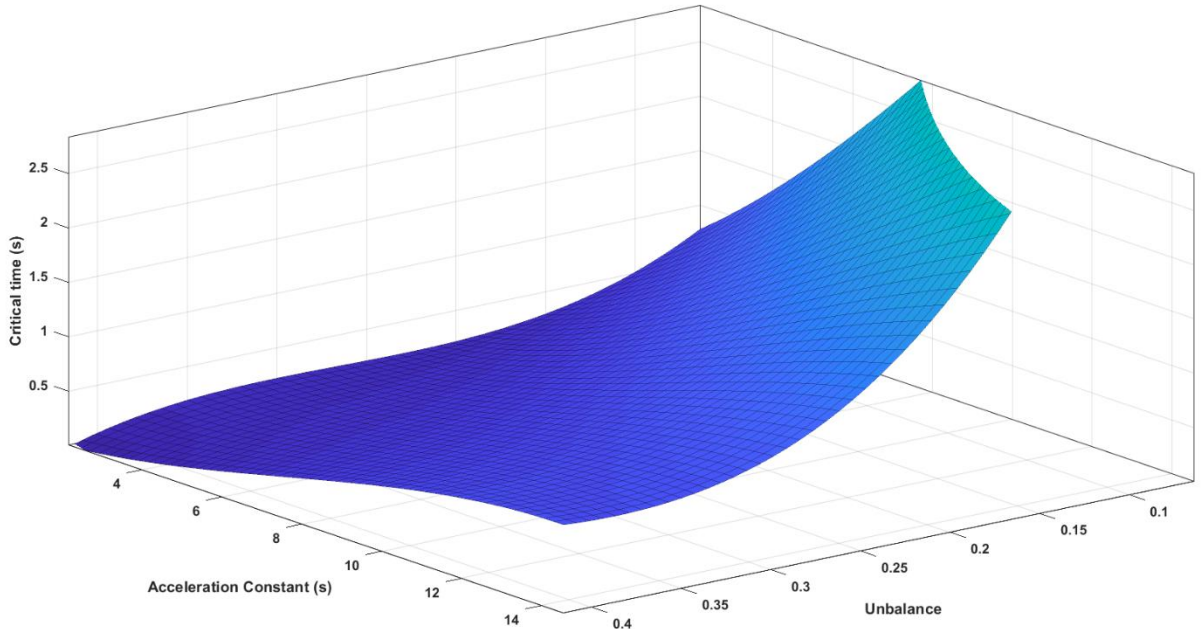


Figure 4-1: Critical time as function of acceleration time constant and load imbalance.

For a better observation of the results; the critical times for specific system acceleration time constants are presented in **Figure 4-2**.

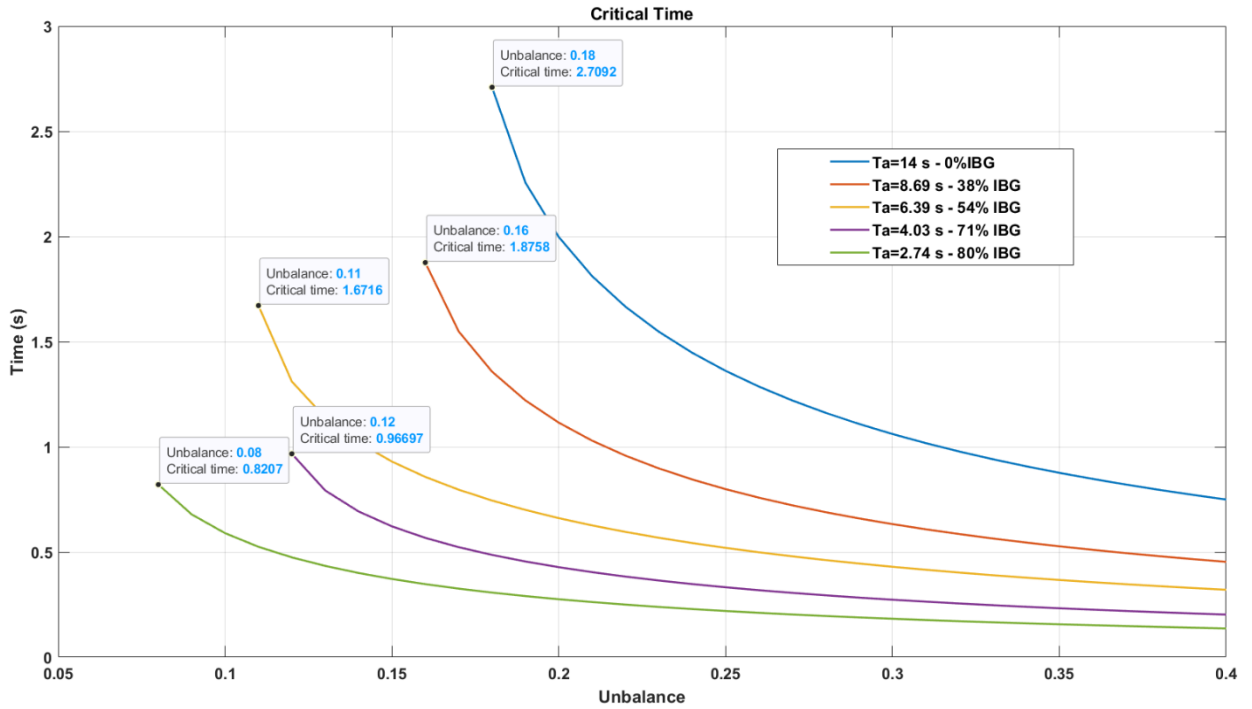


Figure 4-3: Critical time for specific system acceleration time constants

It can be noticed that in a very adverse case scenario; which corresponds to a penetration of inverter based generation of 80% (system acceleration constant of 2.74 s), the UFLS starts with an imbalance of 8% of the load. In this specific case, the critical time to deploy the inverter based fast reserve is 0.82 seconds. Whereas for an imbalance of 40% the available time is 0.14 seconds. With the results obtained from the simulations of the simplified block model, a regression was performed to relate the critical time and RoCoF. The form of the obtained curve is a rational function.

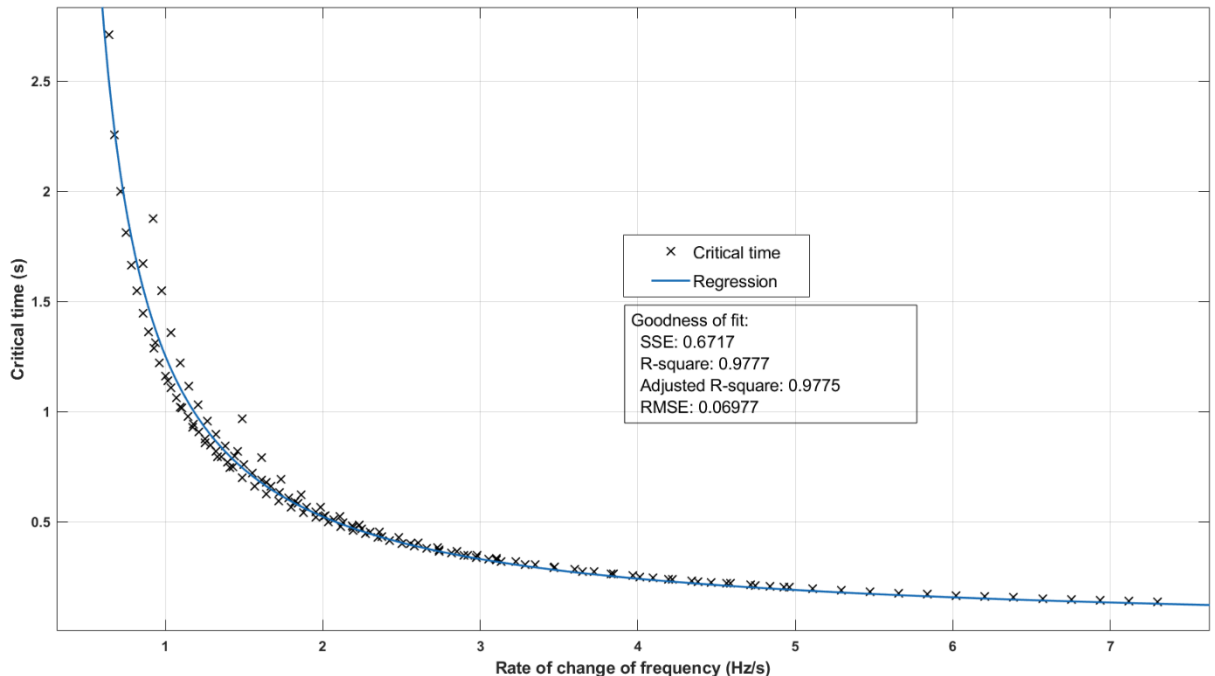


Figure 4-2: Critical time fit as function of ROCOF

Thus the critical time in seconds as function of RoCoF is described in this model by the following equation:

$$t_{cr}(t) = \frac{0.8991}{ROCOF - 0.2824}$$

The frequency nadir when no support is given for inverter based generators is presented in **Figure 4-4**.

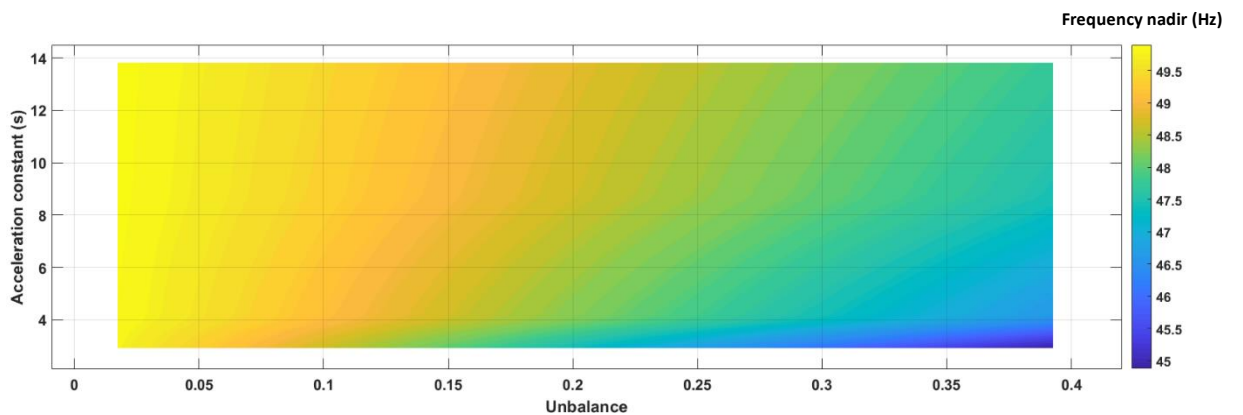


Figure 4-4: Frequency nadir without auxiliary frequency support from IBG.

It is observed how the frequency nadir droops down to 45 Hz for a combination of high IBG and high load imbalance.

Applying IBFPR to the model

With the implementation of equation 3-2; the values of power response from the inception of the disturbance until the critical time are presented in **Figure 4-5** as function of the imbalance and system acceleration constant.

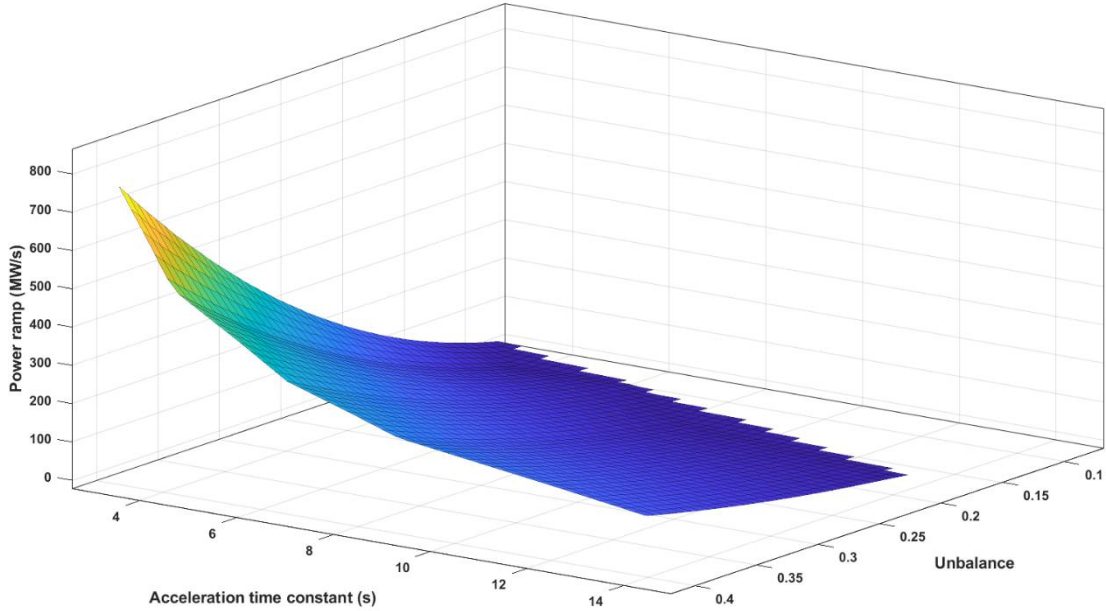


Figure 4-5: Inverter based fast power response ramp

Similarly as it was presented with the critical time, the power ramp is presented in **Figure 4-6** for specific system acceleration constants.

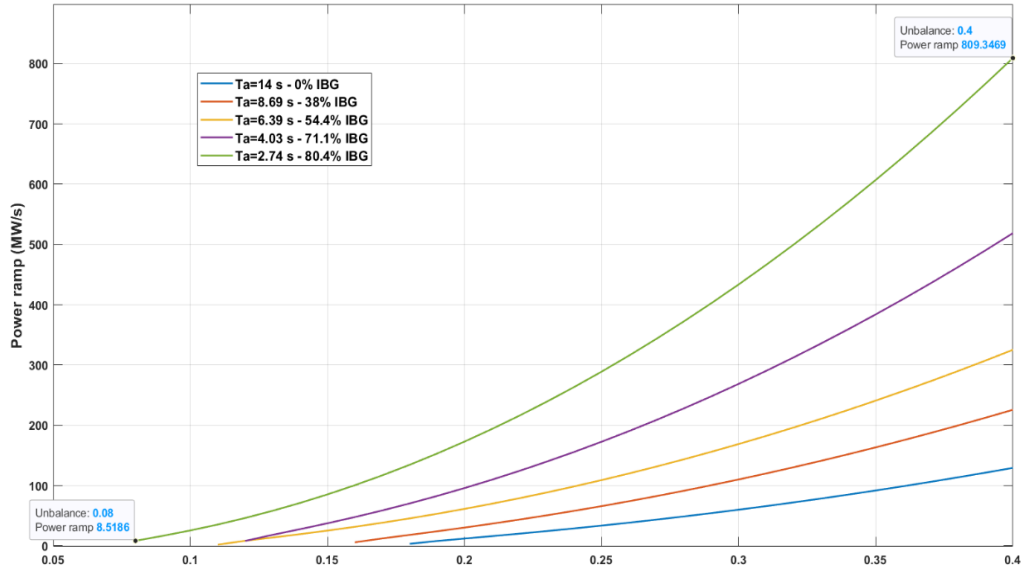


Figure 4-6: IBFPR ramp for specific shares of non-synchronous generation

It can be noticed that for an 80% penetration of non-synchronous generation, a power ramp of 8.5 and 809.35 MW/s are needed to avoid UFLS for imbalances of 8 and 40% respectively.

Applying the resulting ramping power responses to the system an overall improvement is observable. As shown in **Figure 4-7**; the frequency nadir of the system aided by the inverter based fast power reserve barely reach 49.3 Hz.

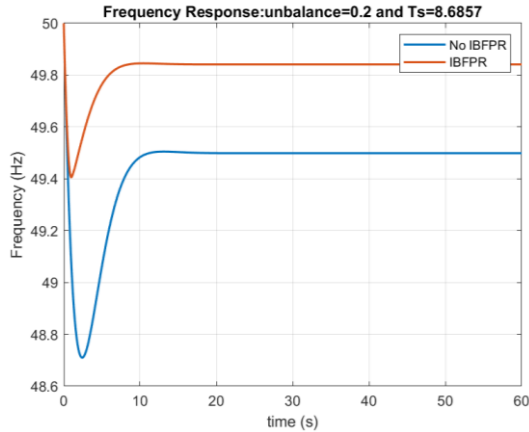


Figure 4-8Frequency response with and without IBFPR for an imbalance of 20% and non-synchronous share of 38%

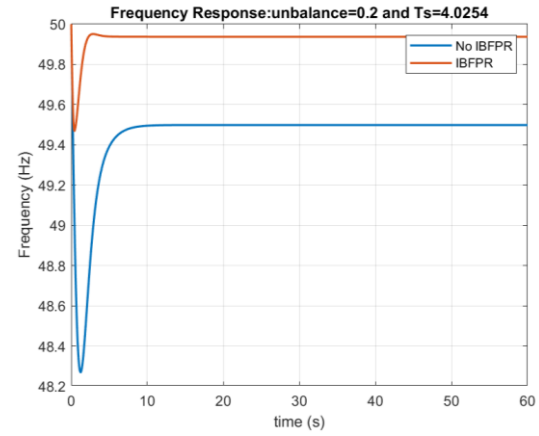


Figure 4-9Frequency response with and without IBFPR for an imbalance of 20% and non-synchronous share of 71%

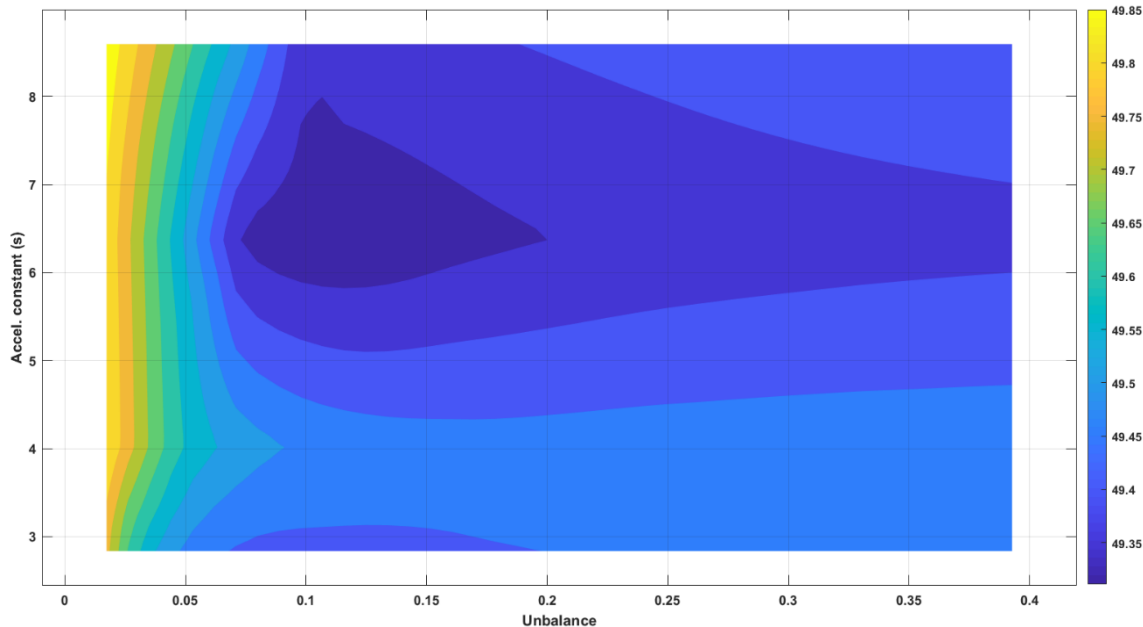


Figure 4-7: Imbalance with the implementation of IBFPR.

Applying only Synthetic Inertia to the System

When the power response of the system is performed solely by the synchronous machines and the decoupled wind turbines are controlled in such a way; that some of the kinetic energy stored in the rotating masses can be extracted when a frequency event takes place, the following frequency nadir characteristic is achieved.

Since inverter based generation is considered to be comprised by wind and PV technologies; the share between wind and PV was considered, in figures **Figure 4-10** and **Figure 4-11** the cases where wind comprises 30 and 60% of the non-synchronous generation were considered, assuming that the total amount of units count with synthetic inertia controls.

For wind power contributions of 30 and 60% of the total inverter based generation, frequency nadir can reach 46 and 46.5 Hz respectively; when the worst imbalance is considered. In any case, UFLS is not avoided for all combination of variables (imbalance and acceleration constant). It can also be observed that frequency nadir under 49 Hz are reached for imbalances bigger than 10% combined with system acceleration constant lower than 8 seconds.

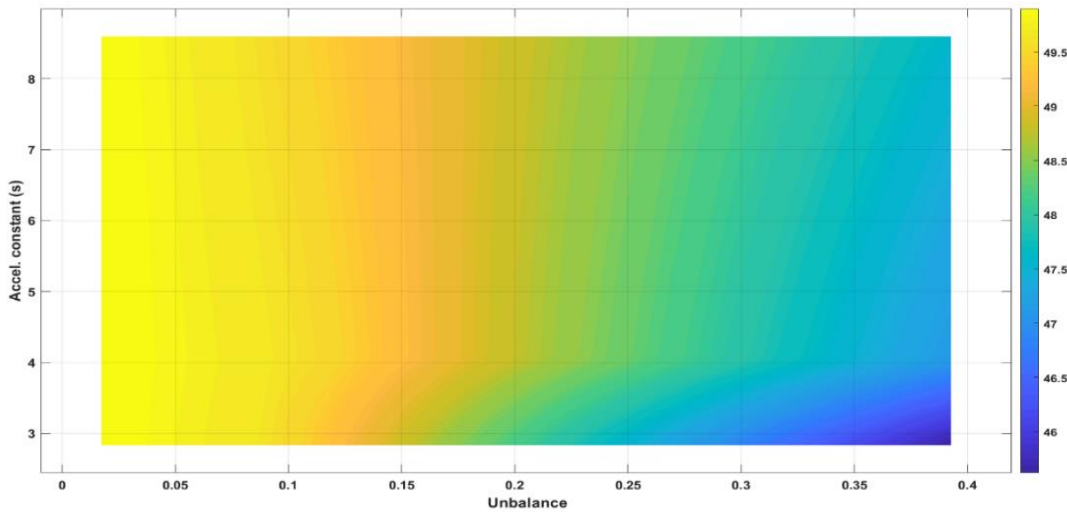


Figure 4-10: Frequency nadir with the only implementation of synthetic inertia; having a 30% of contribution of wind power the total IBG.

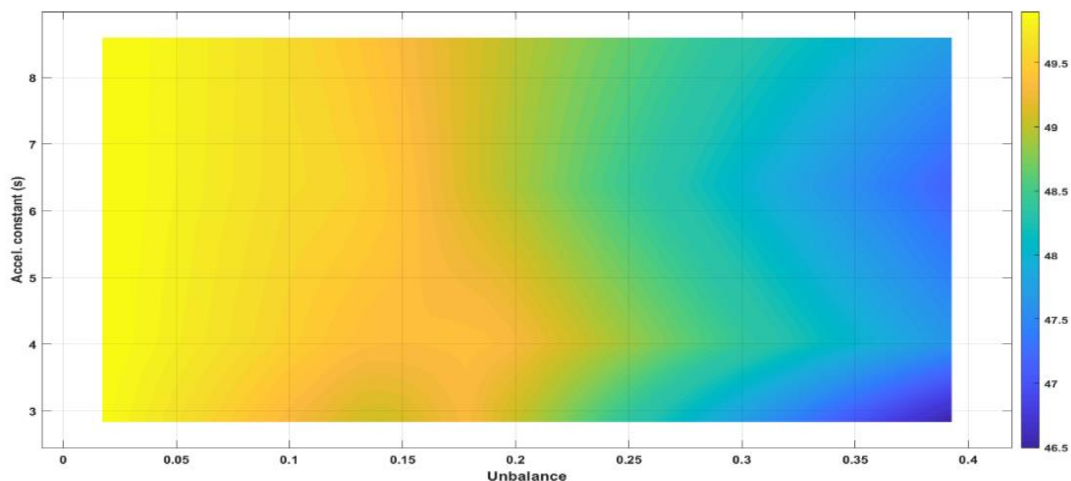


Figure 4-11: Frequency nadir with the only implementation of synthetic inertia; having a 60% of contribution of wind power the total IBG.

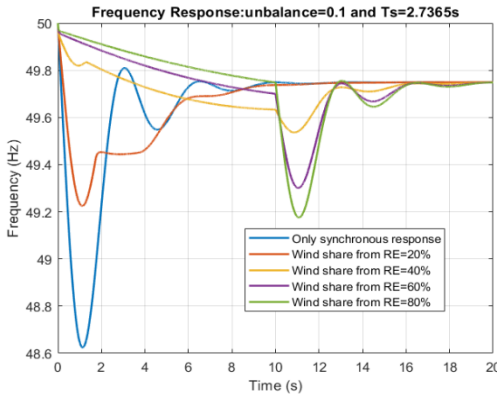


Figure 4-12: Frequency response with only synthetic inertia response and imbalance of 10%

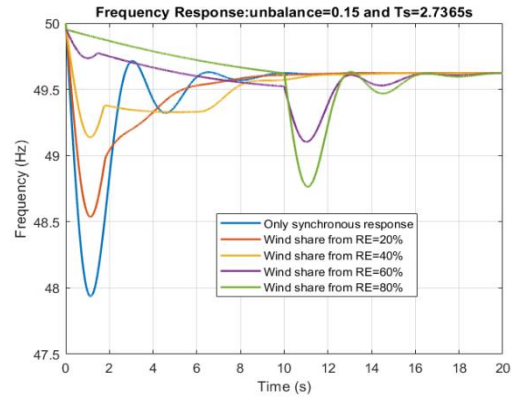


Figure 4-13: Frequency response with only synthetic inertia response and imbalance of 15%

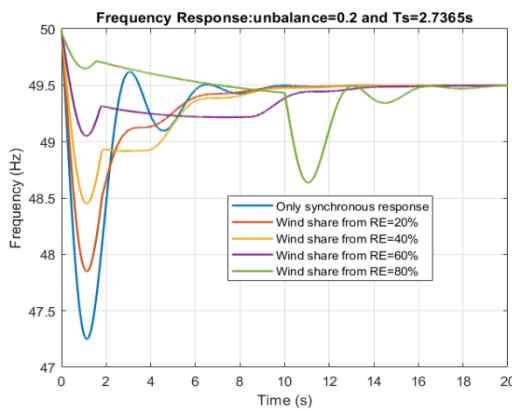


Figure 4-15: Frequency response with only synthetic inertia response and imbalance of 20%

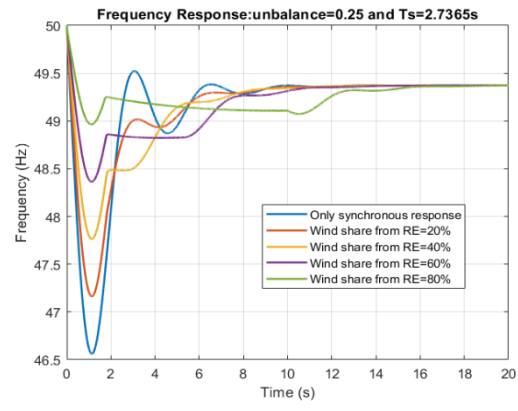


Figure 4-14: Frequency response with only synthetic inertia response and imbalance of 25%

Figure 4-12 to **Figure 4-15** show the frequency response of the system with an acceleration time constant of 2.73 seconds (80% non-synchronous generation) for different load imbalances.

In **Figure 4-12** it can be observed how the frequency drops below 49 Hz with a 10% of imbalance, when no IBFPR or synthetic inertia is used as frequency support strategy. In the same figure, the frequency responses for different levels of synthetic inertia are presented. It is noticed the improvement in the response with the implementation of synthetic inertia with each contribution of wind energy to the non-synchronous generation. UFLS is avoided for every share of synthetic inertia.

As the imbalance increases, the effectiveness of the synthetic inertia decreases, depending on the contribution of wind power to the inverter based generation. **Figure 4-13** shows how contributions of wind power of 40% and 60% from the inverter based generation are capable of avoiding UFLS. Nevertheless the share of 80% begins with a low rate of frequency decrement, the frequency suddenly drops below 49 Hz. This is due to the high amount of synthetic inertial power when compared to the load imbalance. This situation leads to UFLS after the 10 s because frequency has been sustained during that time by the synthetic inertial power. Since 10 seconds is the assumed time limit for exceeding nominal turbine power rate; the synthetic inertial power, which has a big contribution to counteract the power imbalance,

is switched off as depicted in **Figure 4-16** and **Figure 4-17**. On the other hand, when a higher imbalance occurs and the synthetic inertial response is saturated, due to the limitation of 10% of rated power, the mechanical power increases at 10 seconds, having a less severe impact the switching off of the inertial response.

Similar cases are shown in **Figure 4-14** and **Figure 4-15** where it can be seen that the high amount of synthetic inertia response, does not assure stability.

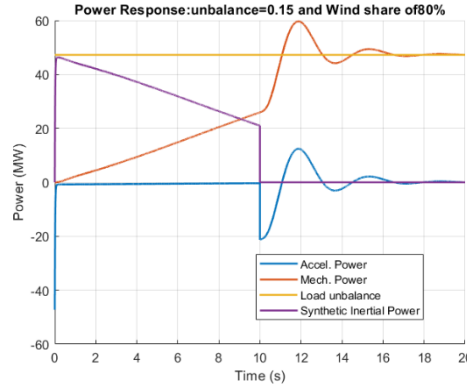


Figure 4-16: Power response

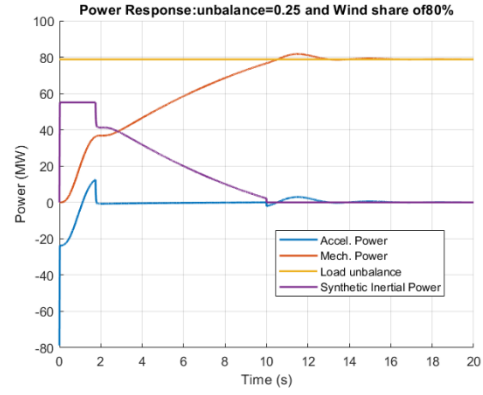


Figure 4-17: Power response

Applying IBFPR and SI

When a combined support from IBFPR and synthetic inertia is implemented in the system an obvious improvement in the frequency nadir is achieved. **Figure 4-18** shows the frequency response of the system with only synthetic inertia from wind turbines whereas **Figure 4-19** incorporates IBFPR as well.

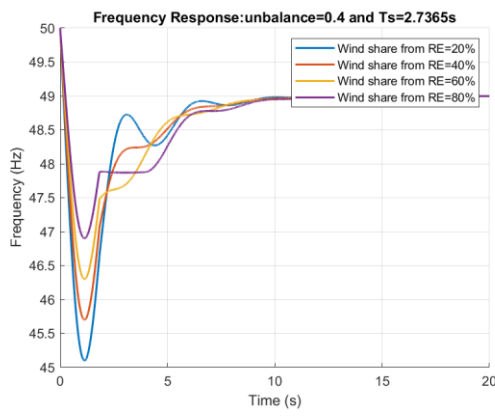


Figure 4-18: Frequency response with only synthetic inertia support.

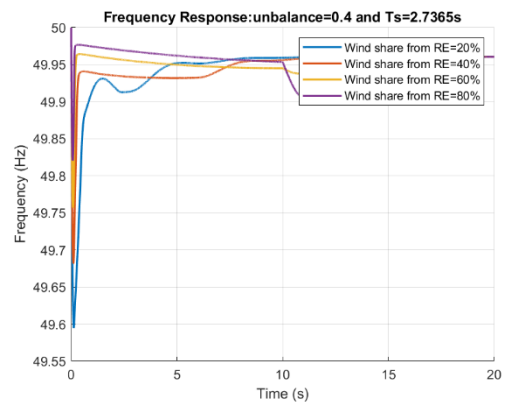


Figure 4-19: Frequency response with IBFPR and synthetic inertia support

Influence of frequency measurement time delay

It was pointed out in chapter 2 the relevance of frequency time measurement in the frequency support response from inverter based generation. The expression obtained for power ramp in chapter 3 did not consider any delay, therefore, the application of the same power ramps to the same combination of acceleration time constant and imbalance was simulated but with an intentional delay added in order to emulate the required time for frequency measurement. **Figure 4-20** and **Figure 4-21** present the results for the frequency nadir when a delay of 100 ms and 200 ms is introduced to the system.

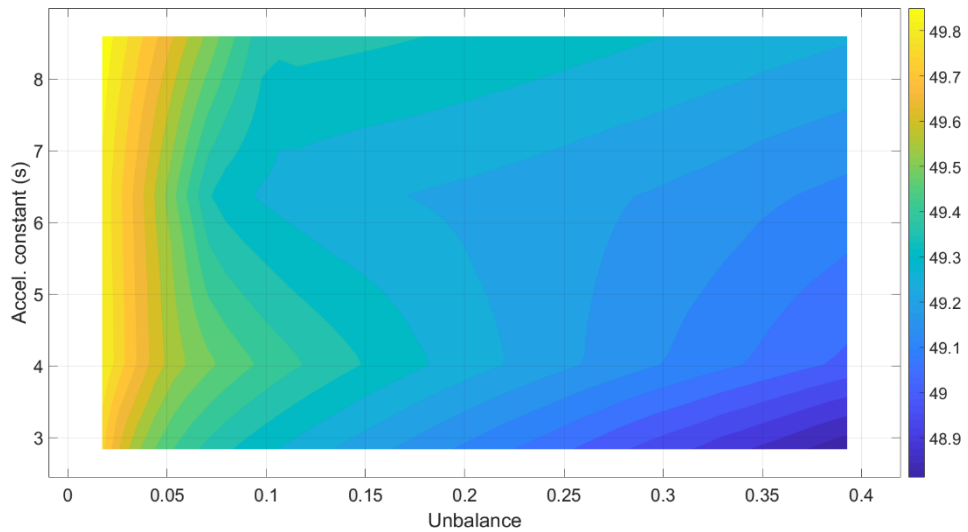


Figure 4-21: Frequency nadir with IBFPR delayed 100 ms.

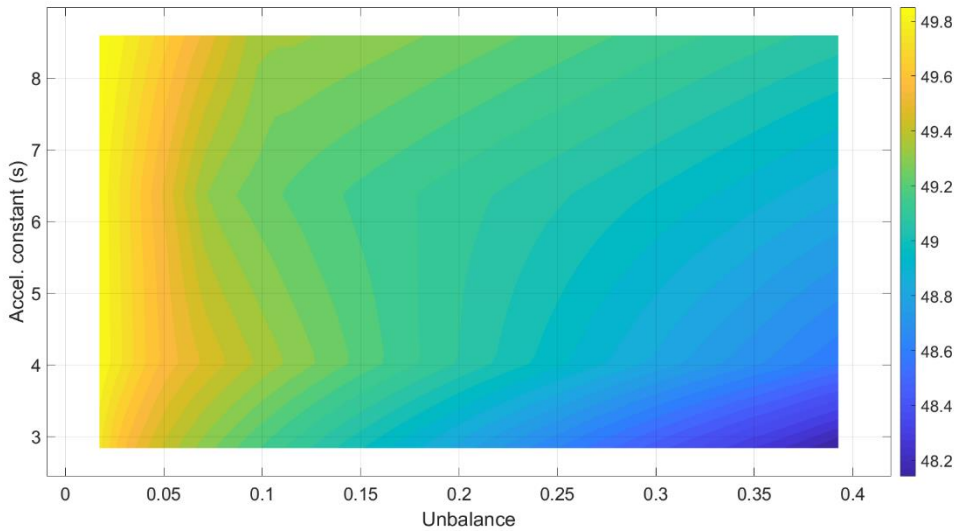


Figure 4-20: Frequency nadir with IBFPR delayed 200 ms.

In the figures above only IBFPR and synchronous reserve were considered. Although UFLS is avoided in a wide range of combinations, stability is not assured when time delay is not taken into account when the ramping response is calculated.

Figure 4-22 shows frequency nadir for specific acceleration constants when no delay is considered, on the other hand **Figure 4-23** and **Figure 4-24** show in more detail the cases with the delay incorporated to the system for the same acceleration constants.

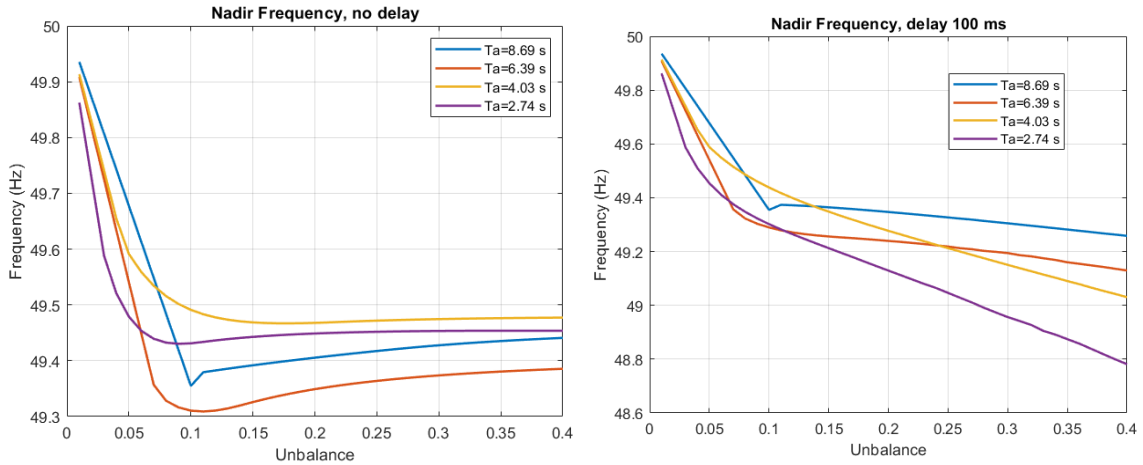


Figure 4-22: Reference frequency nadir with no delay of IBFPR.

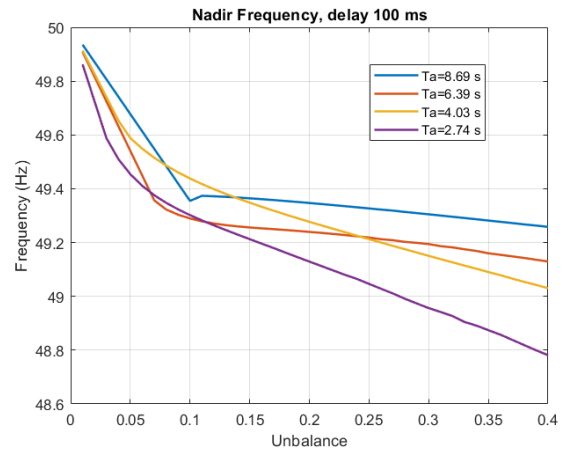


Figure 4-23: Frequency nadir with IBFPR delay of 100ms.

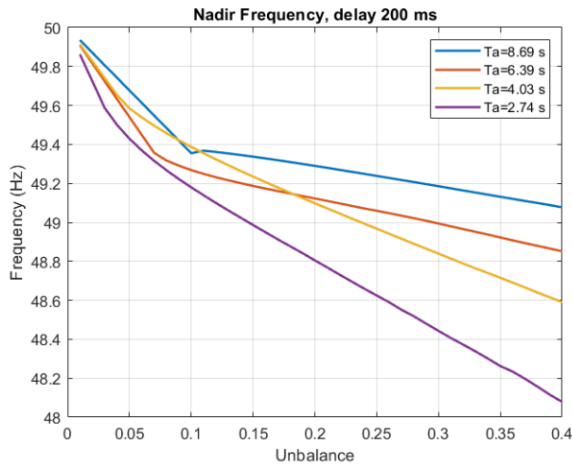


Figure 4-24: Frequency nadir with IBFPR delay of 200ms.

When a delay of 100 ms is considered, the UFLS would occur with 27.5% load imbalance when an acceleration time constant of 2.74 s governs the system.

If a delay of 200 ms is introduced to the system, UFLS would start with load imbalances bigger than 23% and acceleration constants lower than 4.03 s (70% inverter based generation).

Micro-grid Case- SIMSCAPE IEEE 9 bus model

In the SIMSCAPE model all the dynamics of the machines were considered as well as the characteristics of transmission lines and transformers.

Figure 4-25 illustrates the critical times when this model is simulated.

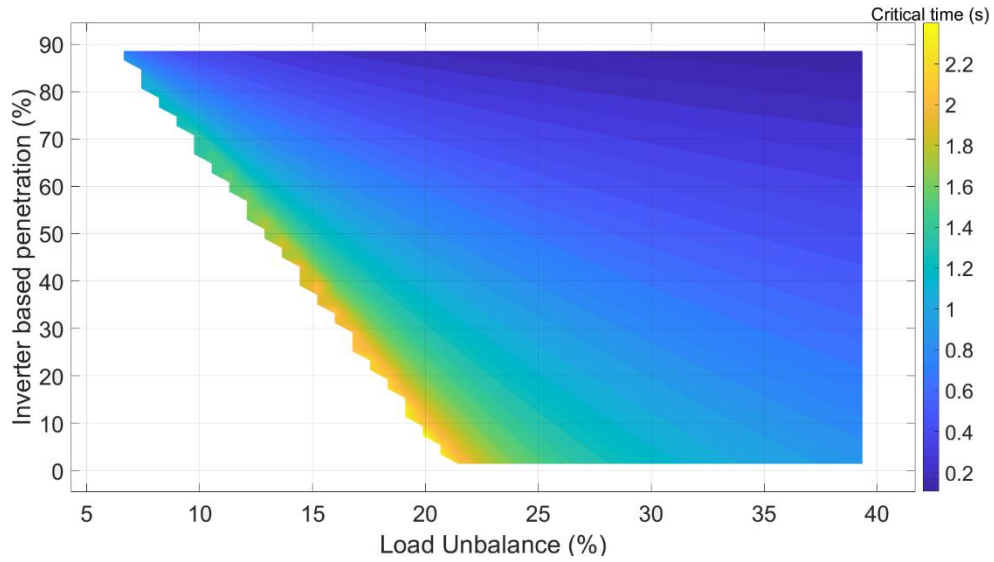


Figure 4-25: Critical time for SIMSCAPE IEEE model.

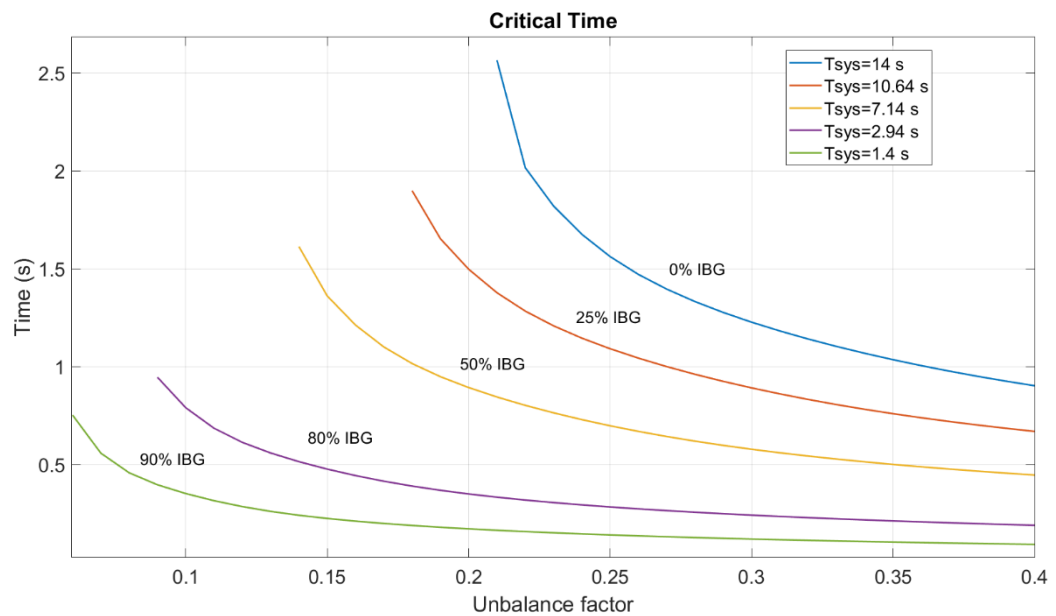


Figure 4-26: Critical time for specific penetrations levels of IBG for SIMSCAPE IEEE model..

When the values of maximum RoCoF are related to the critical time, a regression can be performed. **Figure 4-27** depicts the relation between RoCoF and the critical time.

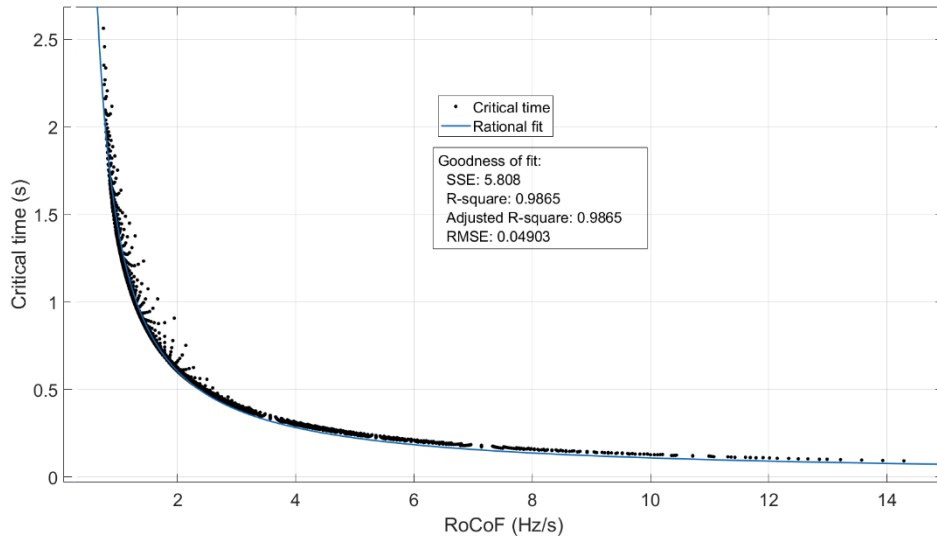


Figure 4-27: Critical time as function of RoCoF.

From the regression the following expression is obtained to relate RoCoF and critical time:

$$t_{cr} = \frac{1.056}{RoCoF - 0.2528}$$

Figure 4-28 shows a comparison between the values of critical time of the simplified IEEE 9 bus model and the critical time calculated with the SIMSCAPE representation of the grid. Relative error for critical time can reach values higher than 34%.

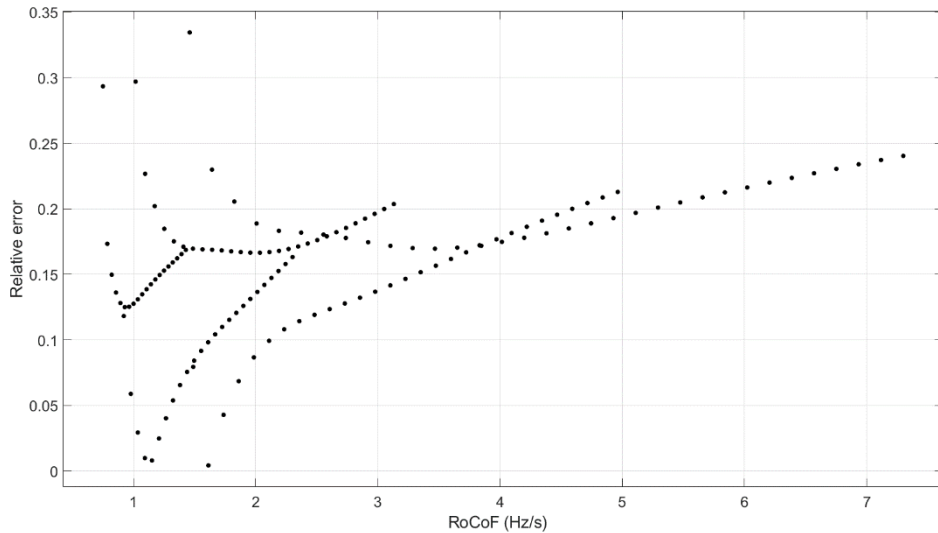


Figure 4-28: Relative error of critical time. Comparison between the SIMSCAPE model and the simplified block model.

The values for the frequency nadir of the system with no support from inverter based generation is shown in **Figure 4-29**. The values shown correspond to the lowest value of frequency reached during 30 seconds of simulation.

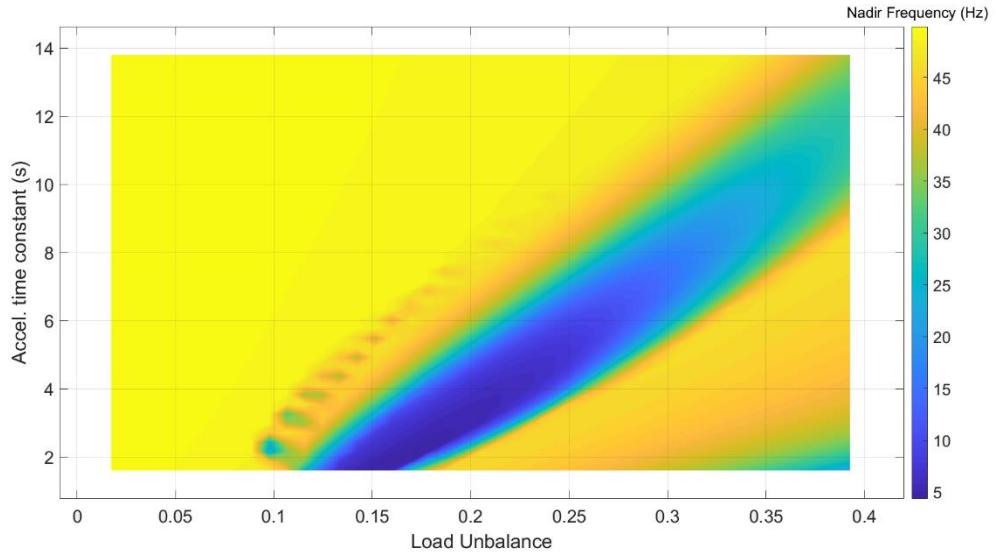


Figure 4-29: Frequency nadir with no additional frequency support

In the same manner as the IBFPR was implemented in the simplified approach of the IEEE 9 bus model, the IBFPR is again added to the system to evaluate frequency response. **Figure 4-30** shows the values of frequency nadir with IBFPR in operation.

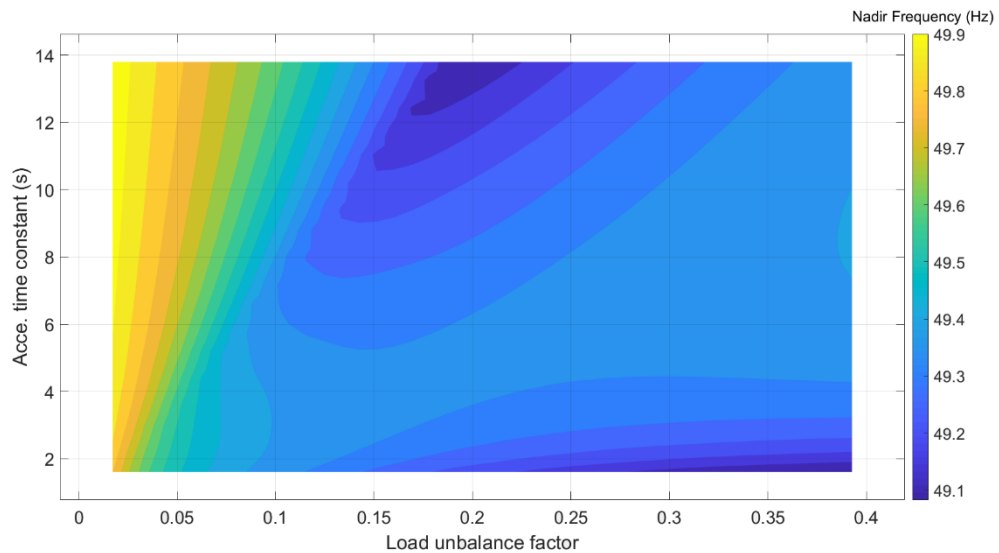


Figure 4-30: Frequency nadir with the implementation of IBFPR.

Figure 4-31 to **Figure 4-34** exhibit the behavior of the frequency response in both case, when no IBFPR is applied and when it is implemented.

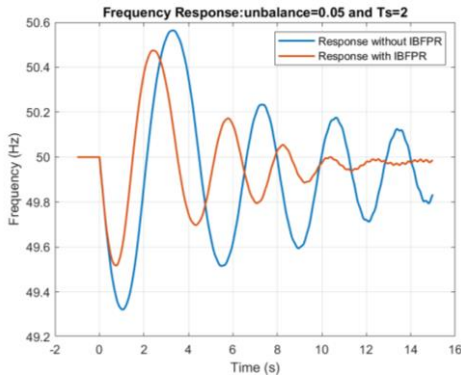


Figure 4-34: Frequency response with 5% of load imbalance and 2 s acceleration constant (85% IBG).

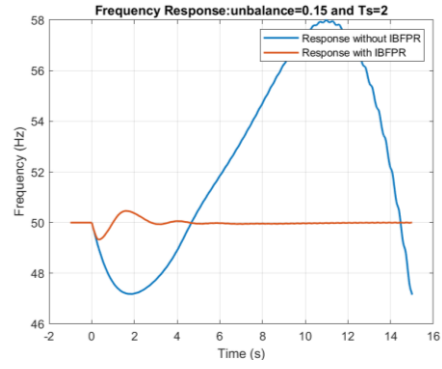


Figure 4-33: Frequency response with 15% of load imbalance and 2 s acceleration constant (85% IBG).

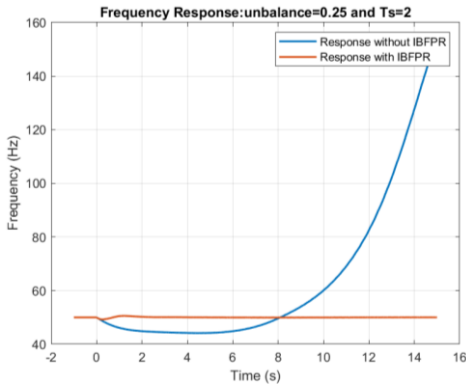


Figure 4-32: Frequency response with 25% of load imbalance and 2 s acceleration constant (85% IBG).

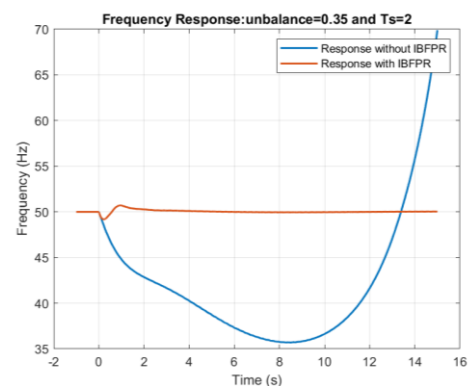


Figure 4-31: Frequency response with 35% of load imbalance and 2 s acceleration constant (85% IBG).

In the figures it can be noticed how the frequency does not stabilize (assuming the frequency it is allowed to have the shown amplitud excursions) when no extra power, besides the one synchronous machines, is injected into the system.

Figure 4-35 shows in more detail the frequency response of the system with an acceleration constant of 2 seconds (85% of inverter based generation) when subjected to load imbalances of 5, 15, 25 and 35%.

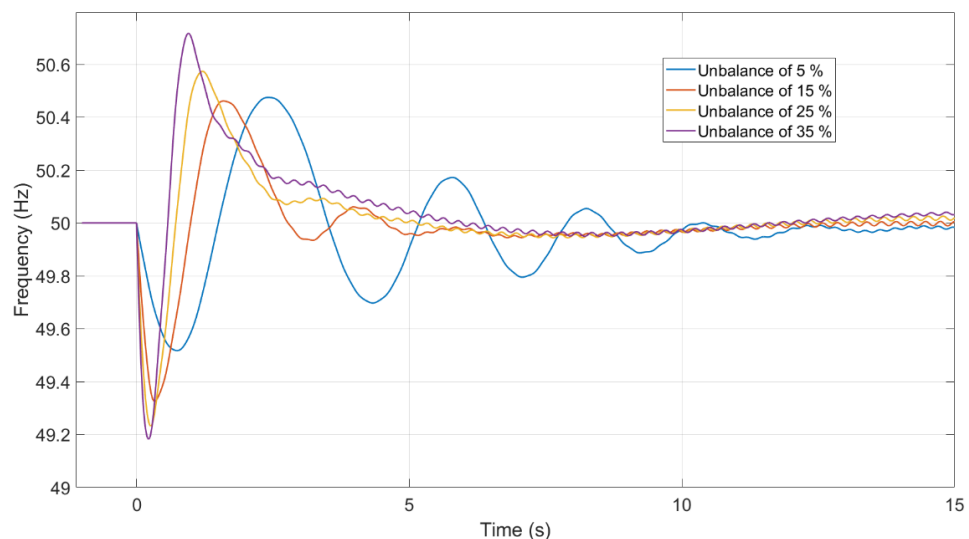


Figure 4-35: Frequency response with an accel. time constant of 2 s (85% IBG) for different levels of imbalance. IBFPR is implemented.

European Island Case

Determination of critical time

In the European island case, the system response characteristic for the interconnected scenario of ENTSOE was assumed to be the same response of each of the resulting islands after an incident leading to splitting occurs. **Figure 4-37** and **Figure 4-36** depict the critical times for IBFPR response.

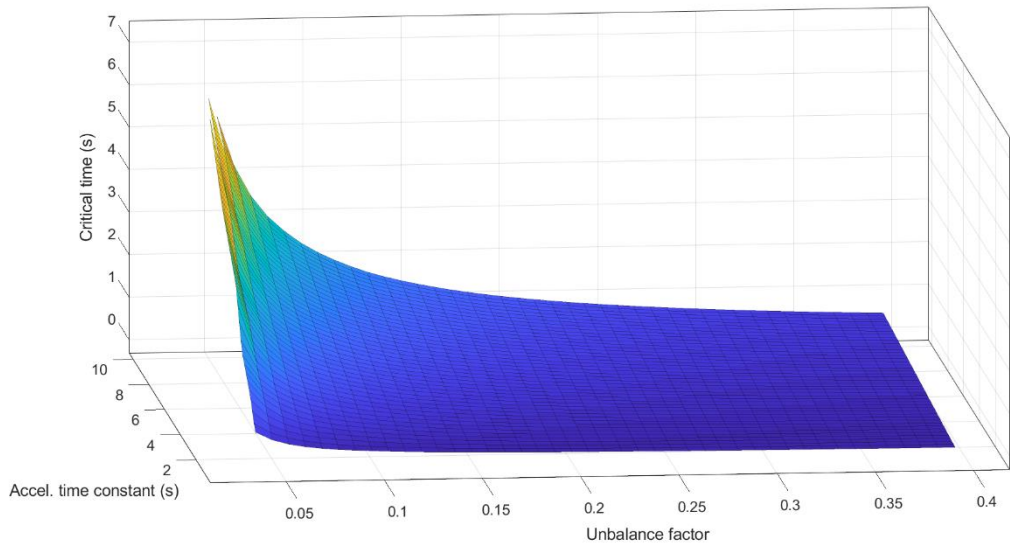


Figure 4-36: Critical time in an electric island in the European power system.

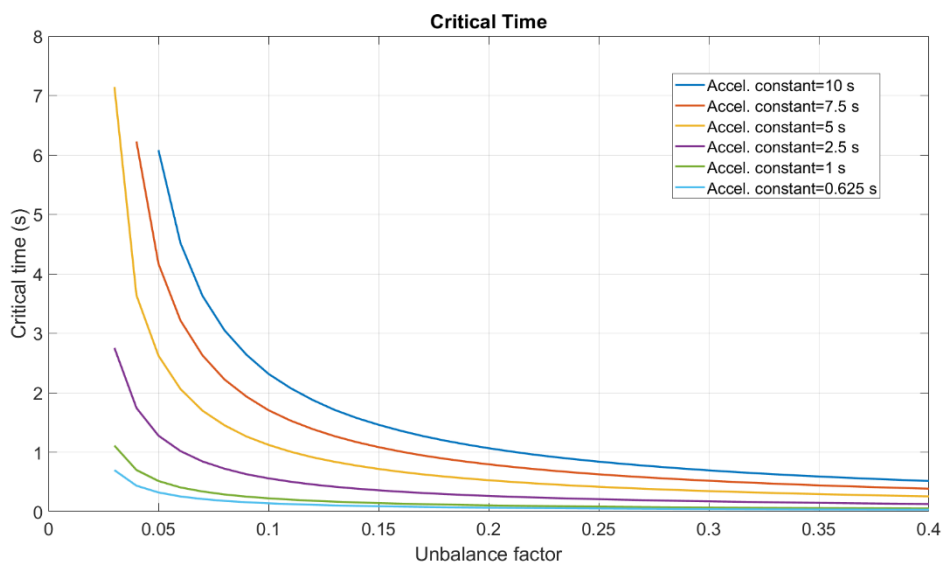


Figure 4-37: Critical time for specific penetrations of IBG.

From the figures it is noticed that for highly imbalanced conditions, critical time starts at approximately 500 ms for almost any system accel. time constant. **Figure 4-38** provides a better visualization for high imbalanced scenarios.

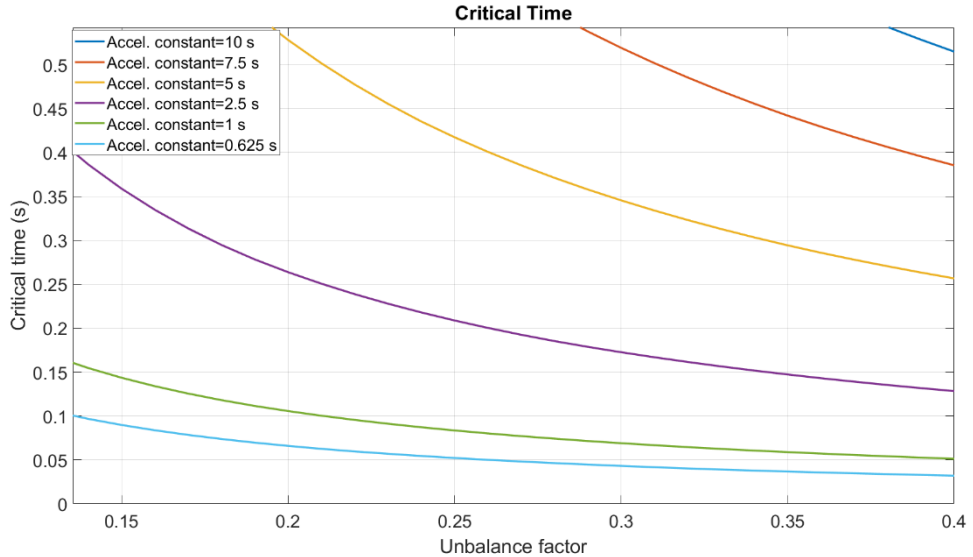


Figure 4-38: Critical time in highly imbalanced conditions.

The relation between critical time and ROCOF is given by the [equation xxx](#) obtained as shown in **Figure 4-39**:

$$t_{cr} = \frac{1.056}{|RoCoF| - 0.2528} \text{ (Seconds)}$$

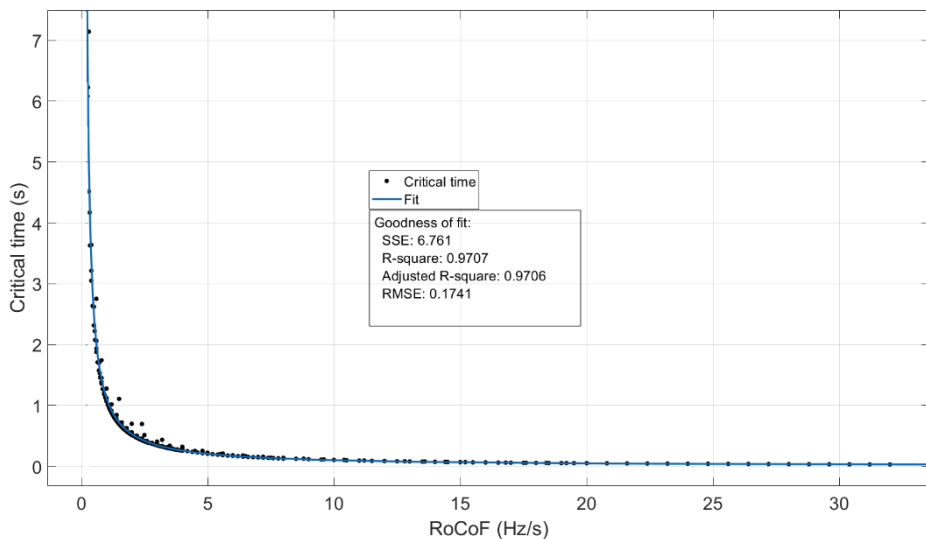


Figure 4-39: Critical time fit as function of RoCoF

Allowing the simulation to run, even though when the values of frequency reach 49 Hz or less; the lowest value of frequency according to the inertia scenario and load imbalance is illustrated in **Figure 4-40**.

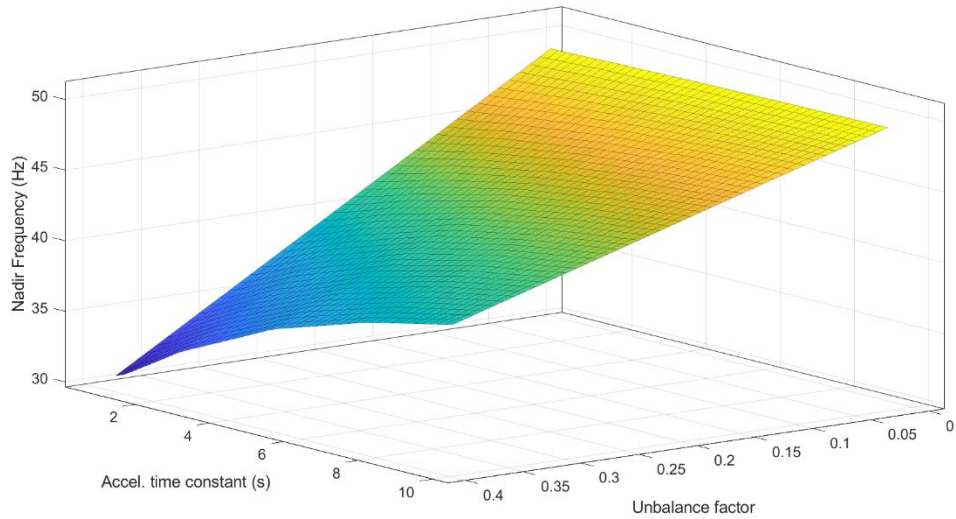


Figure 4-40: Frequency nadir without IBFPR.

Applying IBFPR to the system

When equation 3-2 is evaluated with the values of critical and nadir time for the island scenario; the values of power ramp response from the inception of the disturbance until the critical time are presented in **Figure 4-41** as function of the imbalance and system acceleration constant.

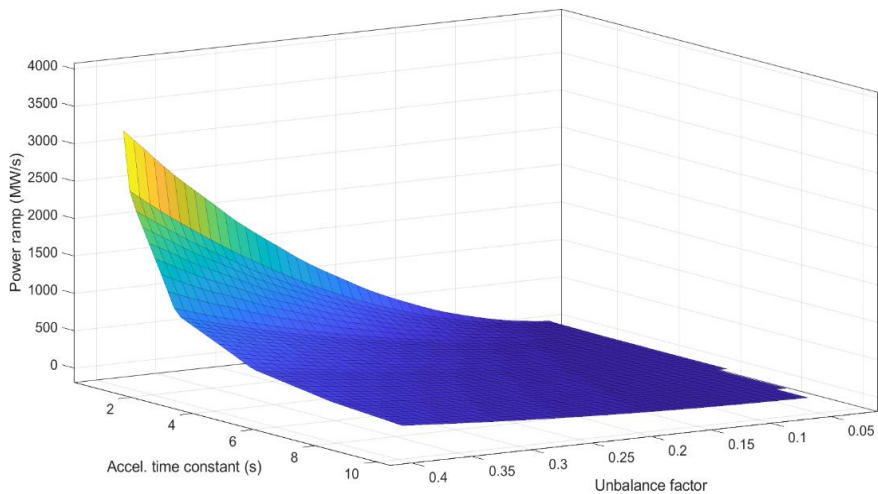


Figure 4-41: IBFPR ramp response in MW/s CHANGE/WRON

It is desirable to obtain results which can be generalized to other inertia scenarios and loads. Hence the same results obtained in **Figure 4-41** are presented in per unit in **Figure 4-42** having as a power base the system power load (150 GW in this case).

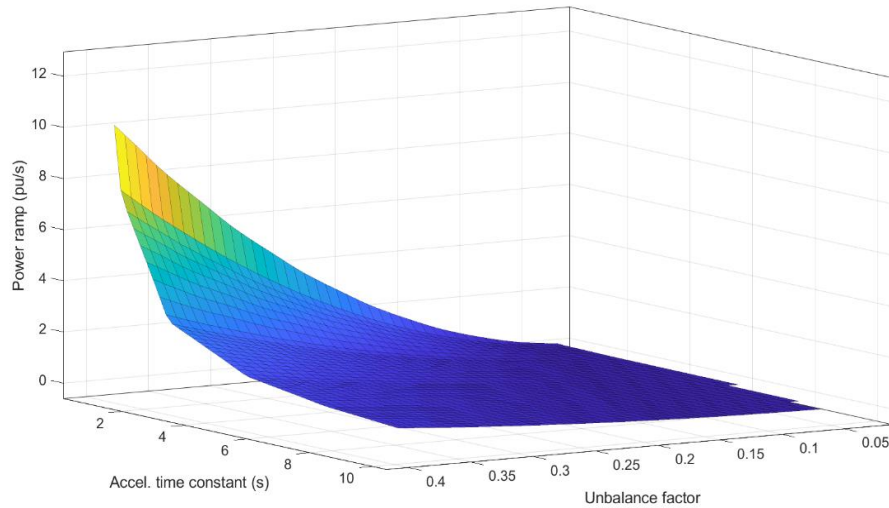


Figure 4-42: IBFPR ramp response in per unit

Once the IBFPR is applied to the system, the following frequency nadir is reached.

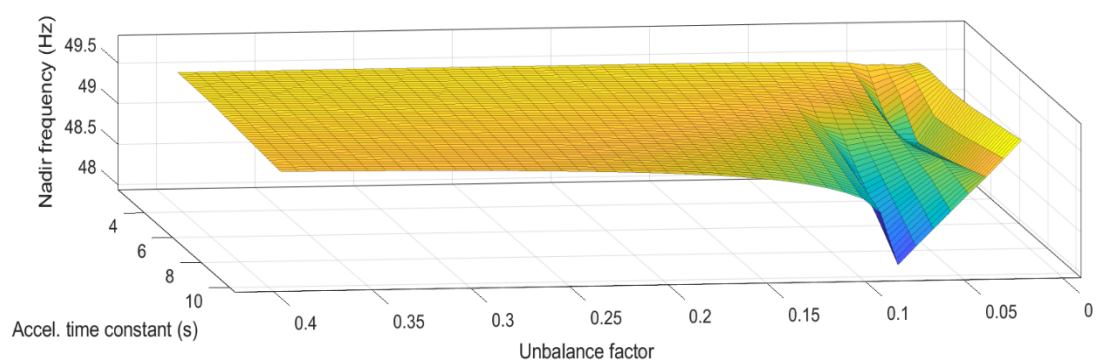


Figure 4-43: Nadir frequency with IBFPR support.

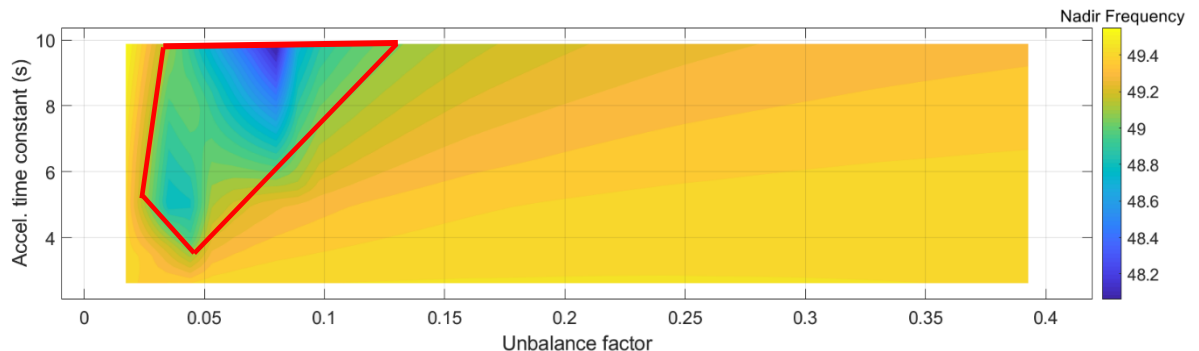


Figure 4-44: Nadir frequency with IBFPR support; UFLS inside the marked area.

In general an improvement in the overall system performance is noted. Nevertheless, as shown in the delimited by the red polygon in **Figure 4-44**; the implemented algorithm is not

able to avoid UFLS. The reason behind is due to the extreme offset in the calculation of the critical time from the fitting function for the RoCoF values corresponding to that area.

Applying only Synthetic Inertia to the System

For the simplified IEEE 9 bus model several contributions of synthetic inertia were simulated and the results of the frequency nadir shown. Synthetic inertia was incorporated as well in the European island model and the frequency nadir values are shown in **Figure 4-45**.

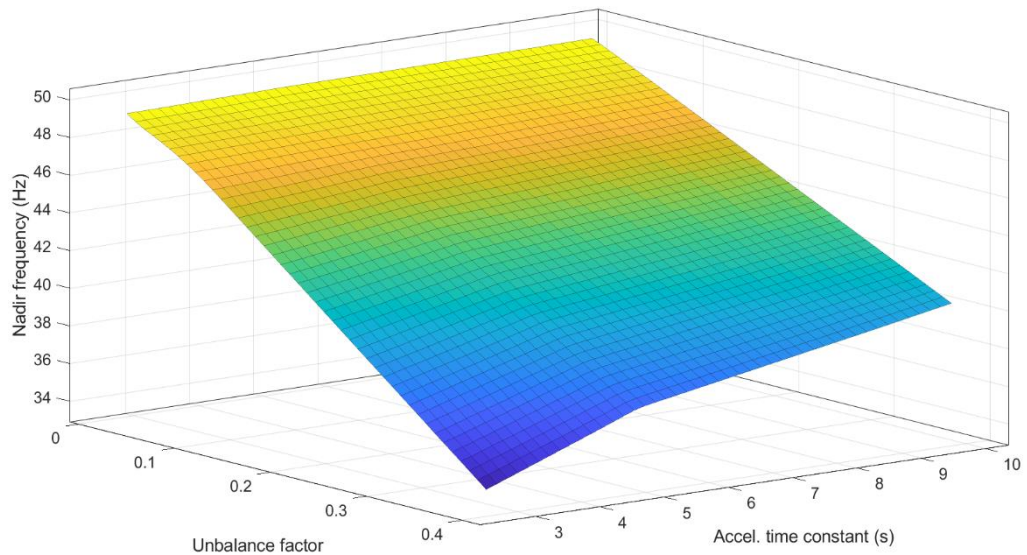


Figure 4-45: Nadir frequency with synthetic inertia support from the 80% of the IBG.

In the same manner than in the simplified IEEE model, the synthetic inertia is not enough for withstanding severe imbalances under high penetration of inverter based generators.

Influence of the frequency measuring time delay

When the same power ramp response is maintained regardless of the inherent delay in frequency measurement, the performance of the system is affected depending on the duration of the delay. **Figure 4-47** and **Figure 4-46** show the corresponding nadir frequencies for delays in frequency measurement of 100 ms and 200 ms.

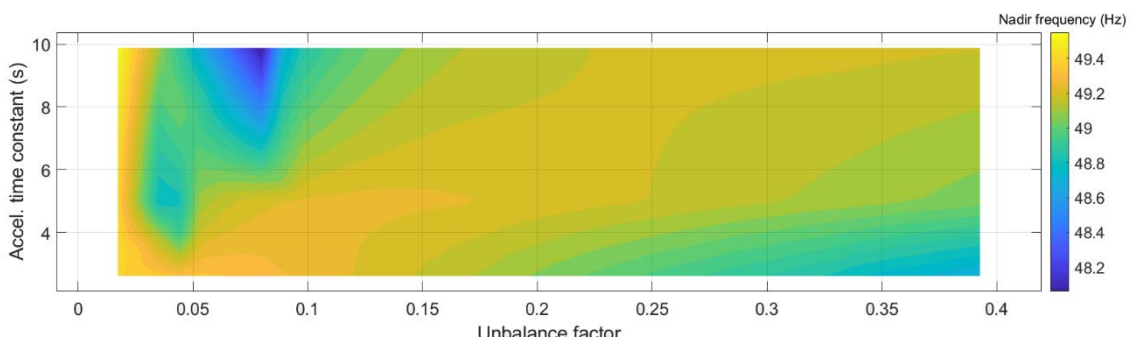


Figure 4-46: Frequency nadir when IBFPR has a delay of 100 ms.

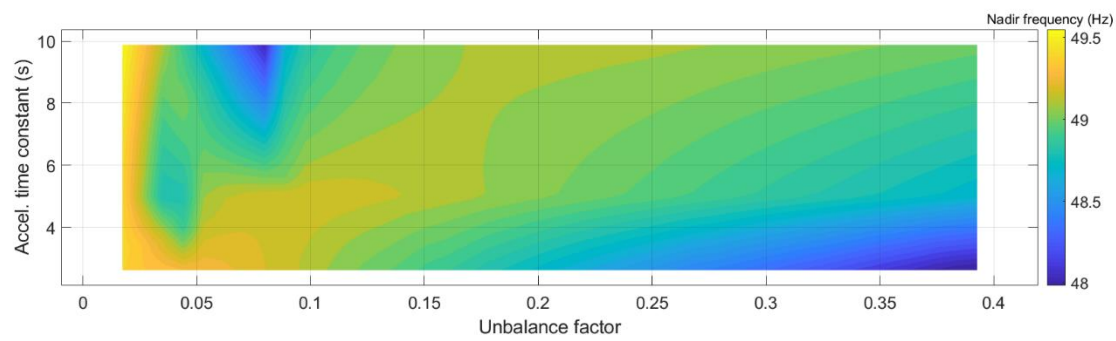


Figure 4-47: Frequency nadir when IBFPR has a delay of 200 ms.

5 Discussion of Results

In this section a deeper look is given to the obtained results out of the simulated cases. In order to allow understandable comparisons between each approach and models; the chapter is divided in three main sections, in which the main results of the simulations will be discussed. This chapter is divided in the following sub-sections:

- Analysis of critical time and implications.
- Analysis of synthetic inertia, fast power response and power reserve implications.
- Synchronizing effect and implications.

Analysis of critical time and implications

Due to the nature of the swing equation, which describes the frequency response in synchronous machines, a reduction of the available time for the inverters to react to perturbations was found as RoCoF increases.

As it was expected, the frequency response is highly dependent on the primary reserve response (governor response). When the IEEE 9 bus model is simplified to one machine and losses are disregarded; critical time deviations from the full dynamic SIMSCAPE model are observed to reach values up to 34%. From the plot of error presented in the result section, it can be observed that the biggest deviations occur at high system acceleration constants and in the low range of RoCoF, allowing primary reserve to take effect. Therefore, it can be stated that the simplifications in the model have a greater influence on the results for low RoCoF and IBG penetration values; in this sense, the simplifications become less significant as the RoCoF increases in such a manner that the activated synchronous primary reserve is not relevant in frequency support.

Despite the discrepancy in the critical time between both approaches in the IEEE 9 bus model; the power ramp calculated for the simplified model and the SIMSCAPE model does not differ from each other in a great manner as exhibit later in **Figure 5-8**. It is then inferred that the discrepancy in critical time estimation is compensated by the factor of nadir time, which due to non-linearity characteristics considered in the SIMSCAPE model, varies upon change in inertia and load unbalance (perturbation); contrary as the linear simplified model in which the nadir time is invariable for perturbations.

In the theory section, the typical frequency measurement time and technologies activation time were discussed. **Figure 5-1** contrasts the critical times obtained from the models with the required time for frequency measurement and full power activation from different technologies.

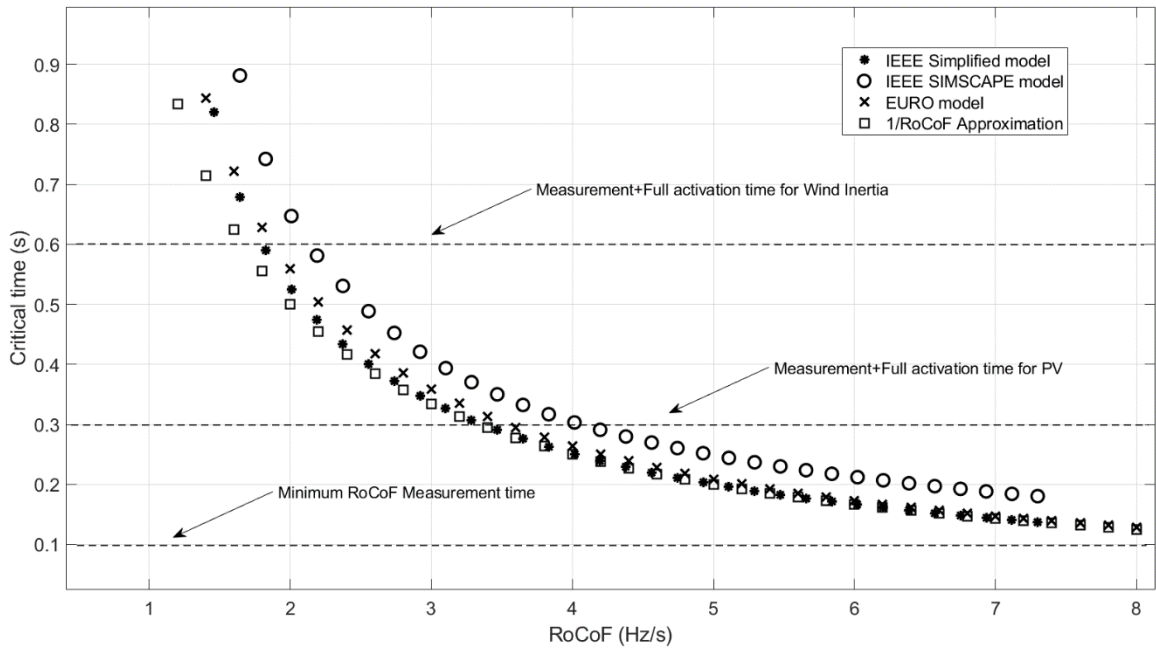


Figure 5-1: Critical time for all scenarios at 80% IBG penetration. Ref

It is observed that in the range higher than 2 Hz/s the critical time trend for the European island and the simplified IEEE model get closer each to other as RoCoF increases. In the same way the SIMSCAPE model for very high values. Therefore, it is inferred that under high RoCoF conditions in any of the models, the primary reserve does not significantly counteract the frequency droop. **Figure 5-1: Critical time for all scenarios at 80% IBG penetration.** Ref. Figure 5-1 demonstrates that primary reserve can be neglected for determination of the critical time when the combination of inverter based generation penetration and load unbalances would lead to high values of RoCoF (>2 Hz/s); as RoCoF increases, the approximation of critical time as $1(\text{Hz})/\text{RoCoF}$ narrows the difference with the results obtained from simulations. Nevertheless such simplification is applicable to the simplified IEEE model and the European island. Hence, the influence of all the dynamics, such as generator exciter, seems to improve the critical time.

Also it is then stated the need of a fast power response to avoid frequency collapse of islanded micro-grid or an electric island in the European scale. Even assuming that power reserve can immediately fully activated after RoCoF reading, the 100 ms limitation is a constraint for high unbalanced islands with high penetration of IBG in the European case as demonstrated in the result section. Additionally, the direct measurement of RoCoF in the 100 ms interval can lead to misleading readings. (GEref)

Analysis of synthetic inertia, fast power response and power reserve implications.

Synthetic Inertia

From the results from the simplified IEEE model and the European island, it can be stated that synthetic inertia from wind turbines do not represent, by itself, a viable way to tackle with frequency transient stability. The reason for its limited capability in contributing to very adverse system conditions is that wind turbines can be overloaded just for a short time (c.a. 10 seconds) with a limited power exceeding the rated power (also c.a. 10% of nominal power). Ref

Since it is expected that most of the inverter based generation will come from inverters connecting wind turbines and PV inverters; it was assumed that a high share of wind power out of the total inverter based generation would successfully contend the frequency droop for light and sever perturbations in the system. Although the results from the simulated scenarios of the simplified IEEE model and the European island show that is not the case.

As already stated, the reasons behind the limitation for avoiding UFLS of synthetic inertia are their operation constraints. In order to illustrate this fact, the same example shown in the result section is brought again to explain how the limitations take place at what moment and circumstances. When the simplified IEEE model is considered under a load unbalance condition of 25% and wind turbine share with synthetic inertia constitutes a 20% of the inverter based generation, which in this case is considered to be the 80% of the total generation. The following power and frequency responses are obtained:

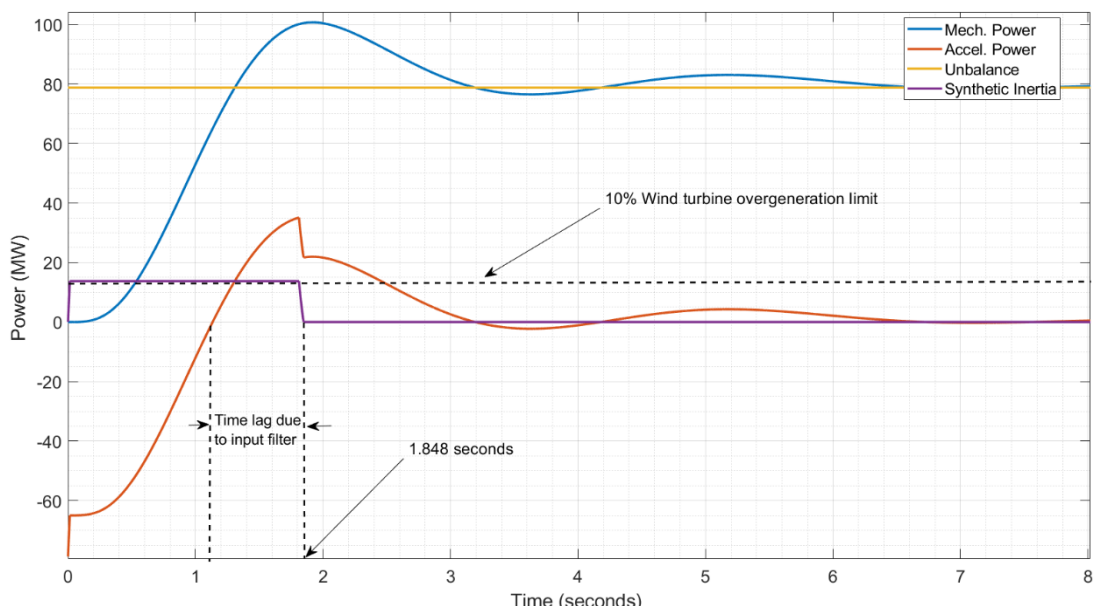


Figure 5-2: Synthetic Inertia power response characteristics of the simplified IEEE model.

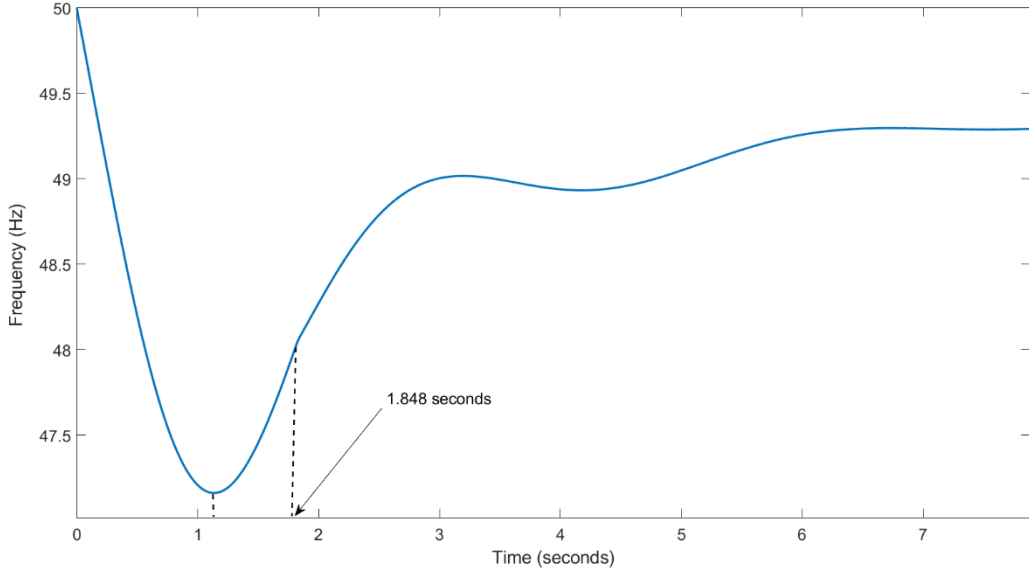


Figure 5-3: Frequency response with 20% synthetic inertia

The limited amount of available synthetic inertial power at the moment of inception of the perturbation causes the system frequency to droop down UFLS, as illustrated in **Figure 5-3**. Since the implemented synthetic inertia model works with the derivative of frequency when a negative load unbalance occurs, meaning that the frequency derivative is negative; once the system RoCoF becomes zero (acceleration power equals zero) the inertia control deactivates. As shown in **Figure 5-2** a delay is observed due to the lag imposed by the filter block in the input of the loop. Similar cases are shown in the result section for different shares of synthetic inertia out of the total inverter based share.

Another big drawback for synthetic inertia is the long activation time required in the order of 500 ms. [ref](#)

Fast power response and power reserve implications

When the power ramp required to meet the power load unbalance at the critical time was calculated in chapter 3; the contribution from the ramping power in diminishing system RoCoF during the inception of the perturbation until the critical time was disregarded. Therefore the fast inverter based power response values at the critical time correspond to the negative accelerating power at that time. Assuming an instant switching of the IBFPR at critical time, the frequency nadir would be 49 Hz (no ramping power before critical time). Nevertheless, a ramp power response was assumed instead. Therefore the calculated power ramp, when applied to the system unbalances, commonly exhibits a frequency nadir higher than 49 Hz, due to the contribution of the ramping period. In this sense, it can be inferred that the longer the ramping period (shorter measuring time), the higher frequency nadir will be obtained. Here again the relevance of the prompt activation in time of the IBFPR. On the other hand, with the faster IBFPR activation, the ramp slope and the steady power output (Inverter based power reserve) can be diminished compromising frequency nadir. In **Figure 5-4** the frequency response of the system is shown when the power response calculated with

equation 3-2 is directly injected in the system. The frequency nadir is around 49.5 Hz. **Figure 5-5** shows the power responses of the system, it must be noted that an inverter based power reserve of 73 MW is required with a power ramp slope of 289 MW/s to achieve such nadir. Since the frequency nadir lays around 49.5 Hz; that would allow a lower inverter based power reserve and a lower power ramp slope as demonstrated in **Figure 5-7** and **Figure 5-6**. Where the inverter power reserved and the power ramp slope are reduced to 58.6 MW and 264 MW/s respectively and frequency nadir reduced to 49 Hz. Both cases considered instantaneous activation of IBFPR at the moment of the incident.

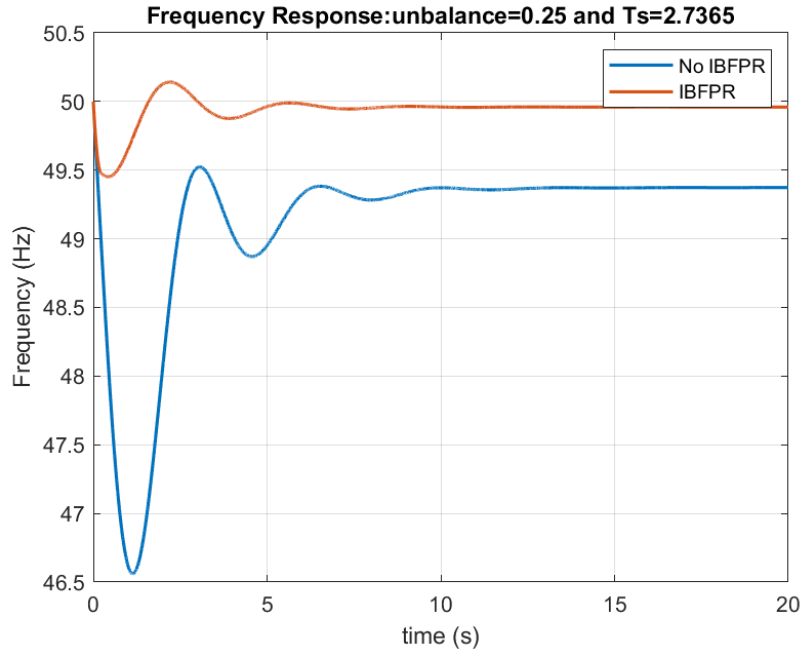


Figure 5-4: Frequency response of simplified IEEE model with injection of calculated IBFPR according to equation 3-2.

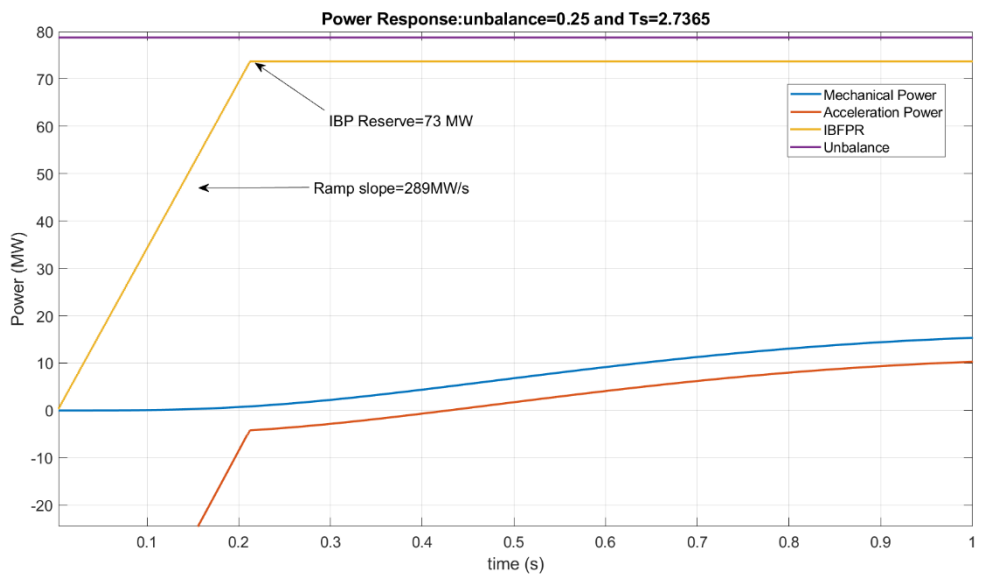


Figure 5-5: Power response of the simplified IEEE model with the injection of the calculated IBFPR.

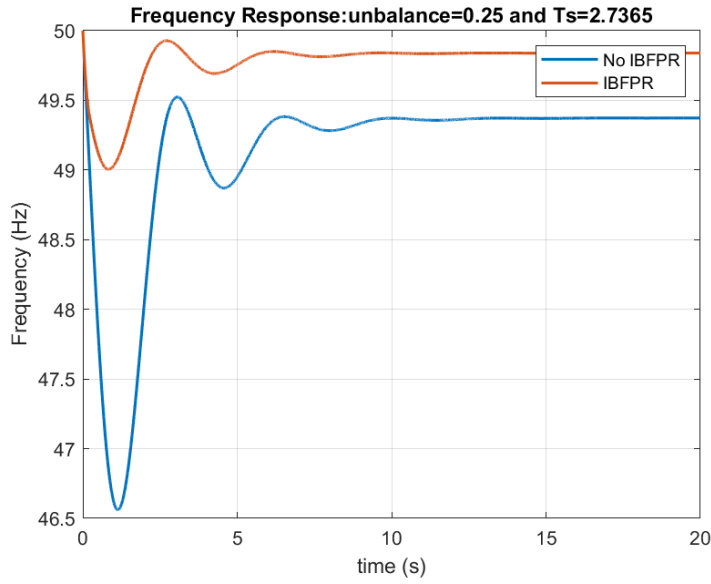


Figure 5-7: Frequency response with an adjusted IBFPR

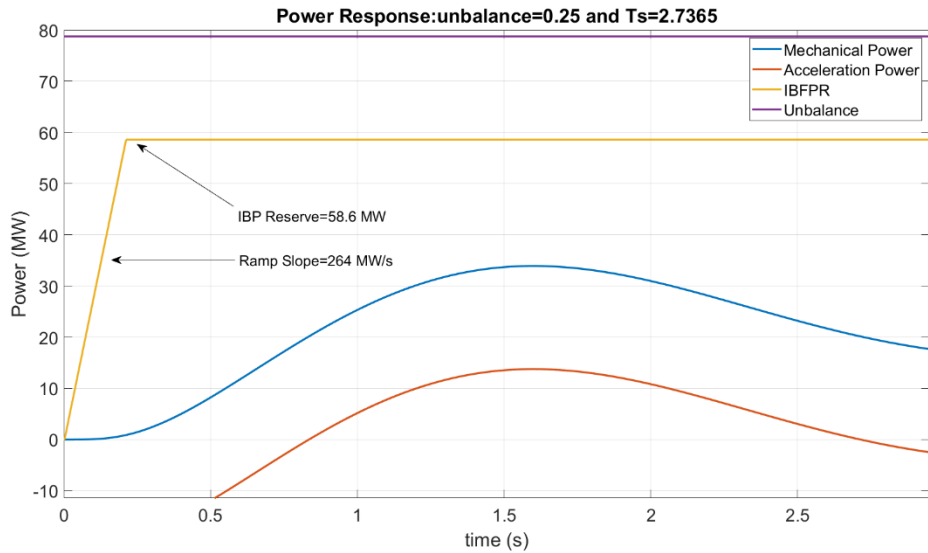


Figure 5-6: Power response needed to have frequency nadir at 49 Hz.

When the activation does not takes place instantaneously, frequency nadir and therefore system stability can be compromised for some combination of system inertia and load unbalance as demonstrated in the result section. In order to assure stability a stepper ramp slope is required in order to meet the required power before critical time. That is achieved by changing equation 3-2 by the adjusted expression:

$$P_{IBFPR}(t) = \Delta P * \frac{\left(1 - \frac{t_{cr}}{t_{nadir}}\right)}{(t_{cr} - t_d)} * t$$

Where t_d is the time delay needed to start the activation of IBFPR.

Power Ramp slope comparisson

When a comparison is established between all the calculated power ramp slopes in per unit (pu)* foot note, It is noted that with high penetration of non-synchronous power in the power system, the required power to ensure no UFLS have a consistent trend between the three models, and a close proximity in the values for RoCoF in the range of 2 to 5 Hz/s is observed between both IEEE models. Such trends can be seen in **Figure 5-8**.

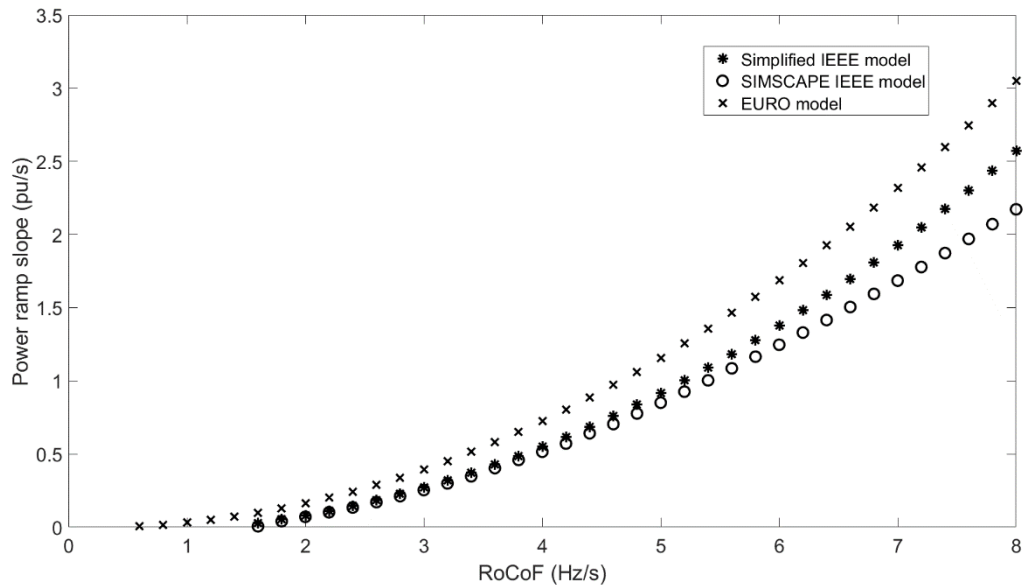


Figure 5-8: Power ramp slope with 80% of IBG penetration.

A bigger amount of power ramp slope is needed in all the range of RoCoF for the European case. After inspecting equation 3-2, it is noticed that the IBFPR is affected by the factor $(1 - t_{cr} / t_{nadir})$, then as nadir time increases, IBFPR increases as well. The nadir time for the European case, due to the action of the self-regulation and primary reserve deployment of 30 seconds, is in the range of 3-12 seconds (6 seconds for 80% IBG penetration) whereas the nadir time for the simplified IEEE model is between 1-3 seconds.

Synchronizing effect and implications.

When the IEEE model was implemented using SIMULINK-SIMSCAPE blocks, in order to incorporate all system component dynamics; system instability was found for low inertia values in the system and due to high unbalances (with no IBFPR). In non-linear systems, the stability is not only determined by the equivalent transfer function but also it is dependent on the inputs or sources ref. In this sense the loss of stability due to huge load unbalances is explained by the non-linearity of the system. When the system is perturbed by a small change in one of the state variables in such a way that the system returns to its initial state or remains close to it; a linearization of the system can be performed and a so called small signal stability analysis can be performed ref.

In the result section it was demonstrated how the SIMSCAPE IEEE model is unstable for unbalances above 15 % with a penetration of non-synchronous generation of 85%, corresponding to a system acceleration time constant of 2.1 seconds. The diminishing of synchronous machines, and the dependency of system frequency and voltage signal from them, lead to a very weak network, where synchronizing and damping torque, which are inherent characteristics of synchronous machines are not enough to stabilize the system (assuming that such excursion of frequency and rotor speed would be allowed to happen) ref. Although the implementation of IBFPR contributes keeping synchronous machine synchronized, low frequency oscillations in the rotor speed/frequency response are observed. This oscillations are created by the lack of damping torque which is provided mainly by the synchronous machines, through damping windings, field exciter and Power System Stabilizer (connected to the machines exciter). For the simplified IEEE model and the European island, only transfer functions describing an equivalent system governor were modeled. Hence in such approaches, the effect and dynamics of synchronous generator's excitors and inter-machine interaction were not taken into account. The before mention factors influence greatly small signal stability ref

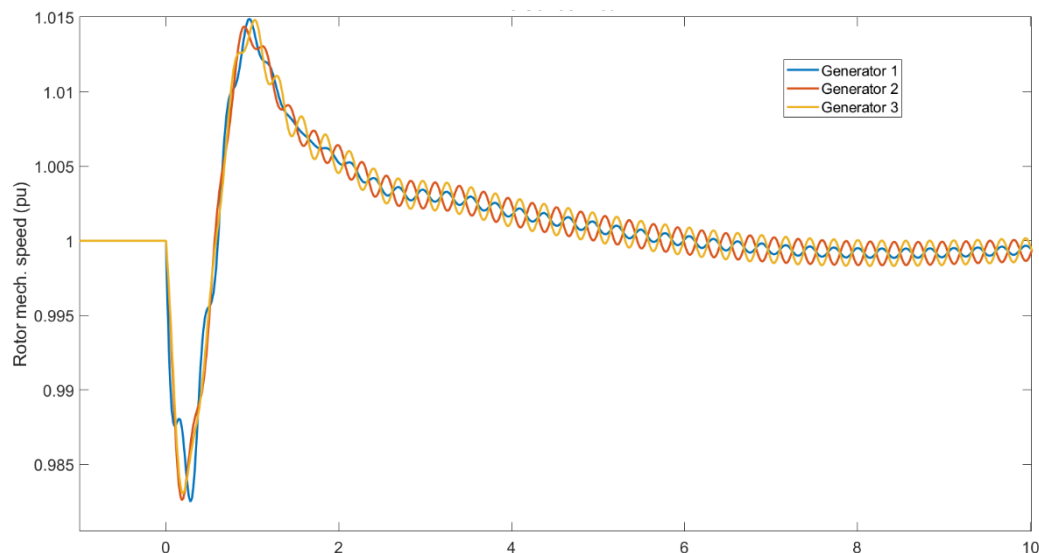


Figure 5-9: Oscillatory effect in rotor speeds in the SIMSCAPE model with 85% IBG and 35% load unbalance and IBFPR support.

Even though the scope of this thesis is to analyze the power-time characteristics needed to avoid frequency collapse; the small signal stability and oscillations associated to big perturbation were observed but they could not be addressed by the simple injection of power to the system. Also in the IEEE model, when a penetration of 95% of inverter based generation and 2% of load unbalance are considered, UFLS is not reached but the system becomes unstable as shown in **Figure 5-10** and **Figure 5-11**. From penetrations levels above 85% complete frequency stability is not ensured with the injection of fast power reserve, only UFLS on the first 10 seconds approximately. Then the system becomes unstable with increasing amplitude oscillations.

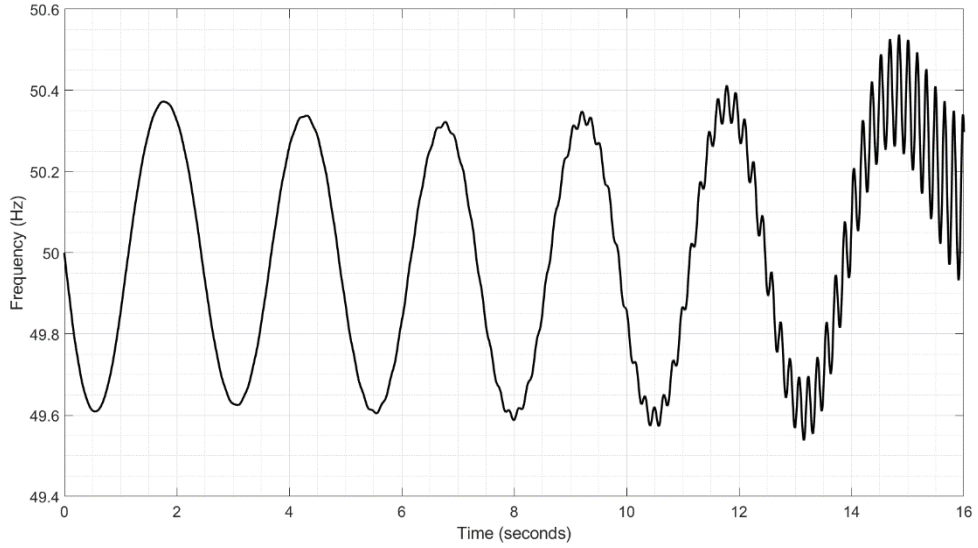


Figure 5-11: Oscillatory behavior from SIMSCAPE IEEE model with 95% IBG and 2% unbalance. No IBFPR is provided.

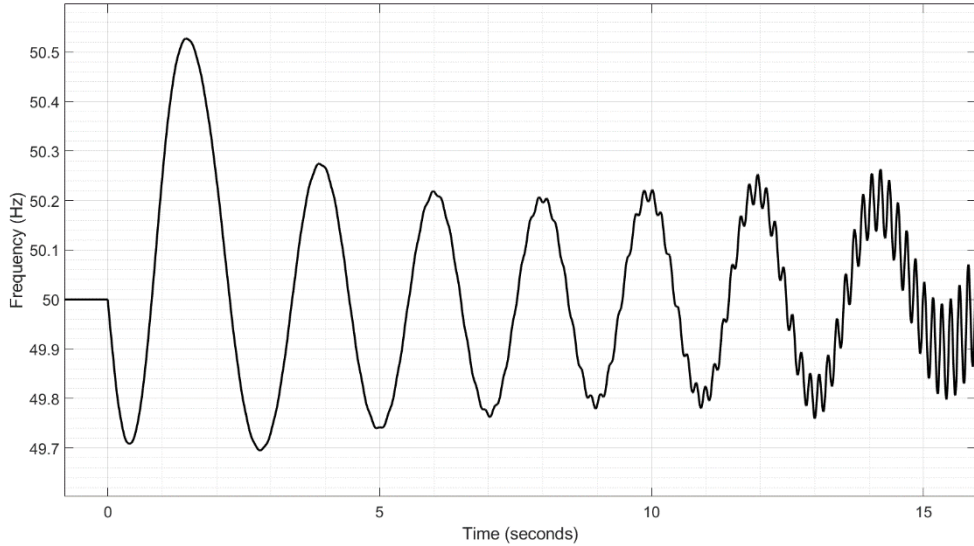


Figure 5-10: Oscillatory behavior from SIMSCAPE IEEE model with 95% IBG and 2% unbalance. IBFPR is provided

It is important to note that ENTSOE in its EUROPEAN interconnected scenario, determined that there is no UFLS when an unbalance of 2 % with high contribution of non-synchronous generation occurs. Nevertheless, no inter-machine interaction was considered and therefore a similar effect as the one in **Figure 5-10** could be experienced.

Conclusions

When a future power system dominated by distributed renewables sources is pictured, it must perform in a reliable way as today's power systems. The increasing amount of power electronic devices facing renewable power sources as PV and wind weakens the power system capability to face perturbation and ensure transient frequency stability. Due to the reduction of system inertia. The natural power output variability of renewables, increasing transmission capabilities between areas, international energy markets and increasing development of micro-grids increase the likelihood of island operation under high unbalanced conditions after a major event. In order to avoid under frequency load shedding under such conditions, inverter based generation must contribute to frequency regulation.

Conventional synchronous machines were found to not be able to ensure transient frequency stability in such conditions. The slow governor operation in the order of seconds is by far too slow to constitute the unique solution for frequency support during the transient period. Inverter based fast power reserve would be needed to be activated in an extreme short time.

To avoid UFLS in penetration scenarios above 80% of non-synchronous generation, inverter based fast power reserve must be deployed over a time in the order of 50-500 ms for load unbalances up to 40%. Nevertheless, today's full power activation time of renewable sources with no storage is in the range of 200 to 600 ms. Hence with today's frequency measuring time and power deployment from renewable sources; load shedding and possible total black outs would not be avoided.

An effective frequency measurement in shorter time would contribute to reduce the amount of inverter based power reserve when the system count with no power storage and therefore, to diminish the de-loading factor needed to provide it, up to a 20%. In order to avoid UFLS, ramping capabilities up to 3 times the power unbalance per second would be required from the inverter based sources; for combinations of inverter based generation above 80% and load unbalance in the order of 30% in both, micro grid and European scale islands. To achieve such response from distributed source, a continuous knowledge of the connected inertia to the system is required by the inverters since the IBFPR is based on the unbalance on the system and the critical time, which depends on system inertia. Additionally, system inertia is the linking bridge between RoCoF and power unbalance determination.

Although UFLS is avoided in scenarios with penetrations of non-synchronous generation above 85% with injection of inverter based fast power reserve; total system stability is not ensured after a few seconds (~ 5 s), due to the presence of undamped oscillations provoked by the poor damping torque present in the system as consequence of synchronous share reduction.

In general, similar behavior is exhibit from the different models and approaches, even though they differ considerably in size and complexity. Hence, simplified block representation of

the power system seems to be a fair way to sketch overall system trends and responses. A comprehensive method for estimation of the inverter based fast power reserve and critical time were developed and proved through the implementation in two main cases.

Outlook

It was demonstrated the need of a fast power reserve for the reliable operation of future's grid. To do so, an accurate and fast estimation of the power grid state is fundamental in terms of frequency and connected inertia; to enable inverter based generation to play a dominant role in frequency support. Further investigation in this area is fundamental to allow flexible inverter based generation. The integration of energy storage systems are promising alternative to provide ancillary services to the grid, the diminishing trend cost and fast activation times could be optimized together with de-loading of renewable sources to provide frequency support.

Investigation of grid forming inverters connected along with synchronous machines and grid-following should be further investigated. So far, investigation and implementation of such type of inverters has been done mostly for stand-alone systems.